The Geological Society of America
Field Guide 64

Paleoproterozoic tectonics of the northern Colorado Rocky Mountains Front Range, USA

Graham B. Baird
Timothy W. Grover
Department of Earth and Atmospheric Sciences, University of Northern Colorado, Greeley, Colorado 80639, USA

Kevin H. Mahan
Michael G. Frothingham
Department of Geological Sciences, University of Colorado Boulder, Boulder, Colorado 80309, USA

Markus B. Raschke
Department of Physics, University of Colorado Boulder, Boulder, Colorado 80309, USA

Andreas Möller
Department of Geology, The University of Kansas, Lawrence, Kansas 66045, USA

Adam S. Chumley
Jacob C. Hooker
Department of Earth and Atmospheric Sciences, University of Northern Colorado, Greeley, Colorado 80639, USA

Nigel M. Kelly
Bruker Nano Analytics, Denver, Colorado 80212, USA

Julien M. Allaz
Department of Earth Sciences, ETH Zürich, Zürich 8092, Switzerland

ABSTRACT

Two models have been proposed to explain continental crust generation in accretionary orogens. One model suggests that accretionary orogens are formed by the successive collision of juvenile arcs. The second model invokes tectonic switching, which is the repeated cycles of slab rollback and extensional backarc basin formation followed by basin collapse caused by collision, shallow subduction, and/or increased convergence rate. The northern Colorado Front Range, specifically in and around the Big Thompson, Rist, and Poudre Canyons, offers excellent exposures of Paleoproterozoic rocks to test which accretionary model best explains crust generation for a portion of the Yavapai Province.

In this contribution we have two goals: The first is to provide a field-trip guide that augments Mahan et al.'s (2013) field guide, which uses many stops that have become

Baird, G.B., Grover, T.W., Mahan, K.H., Frothingham, M.G., Raschke, M.B., Möller, A., Chumley, A.S., Hooker, J.C., Kelly, N.M., and Allaz, J.M., 2022, Paleoproterozoic tectonics of the northern Colorado Rocky Mountains Front Range, USA, *in* Mahan, K.H., and Carpenter, L., eds., Field Excursions in the Front Range and Wet Mountains of Colorado for GSA Connects 2022, p. 39–66, https://doi.org/10.1130/2022.0064(03).

inaccessible or have changed because of catastrophic flooding that occurred in September 2013. This more current guide focuses on a variety of mostly Paleoproterozoic rocks within what some call the Poudre Basin. These rocks include clastic metasedimentary rocks, amphibolite, the Big Thompson Canyon tonalite suite, the northern Front Range granodiorite, granitic pegmatites, and Mesoproterozoic Silver Plume granite. The second goal is to present and synthesize new and existing geochemistry, geochronology, and isotopic data, and then discuss the origins, age, deformation, and metamorphism of these rocks in the context of the proposed tectonic models.

These data were synthesized into the following tectonic model for the Poudre Basin. At ca. 1780 Ma, the juvenile Green Mountain arc, located today along the Colorado-Wyoming border, formed and extended shortly thereafter during slab rollback, resulting in the extensional backarc Poudre basin between the diverging arc fragments. Sedimentation within the basin began at inception and continued to ca. 1735 Ma when basin rocks were intruded by the Big Thompson Canyon tonalite suite and the northern Front Range granodiorite, all of which were subsequently metamorphosed and deformed at ca. 1725 Ma. Felsic magmatism and deformation within the basin were perhaps driven by the northward shallow subduction of an oceanic plateau or seamount. This suggests that following accretion of the Green Mountain Arc, tectonic switching explains formation and collapse of the Poudre Basin and creation of some of northern Colorado's crust.

INTRODUCTION

Continental crust is an integral part of the Earth system and is formed, shaped, and destroyed by a variety of tectonic and surficial processes. These processes, and the state of continental crust at any time, are linked to global climate, life evolution, and the distribution of natural resources. Therefore, it is fundamental to a wide range of Earth science pursuits to understand how continental crust is formed.

One proposed mechanism driving the growth of the continents occurs within accretionary orogens, where "juvenile" island arcs, those built on oceanic crust, are accreted to the margin of a growing continent (Fig. 1). This interpretation is underpinned by the observation that bulk continental crust is geochemically broadly similar to island arc crust (e.g., Taylor, 1967, 1977; Kemp et al., 2009; Hawkesworth et al., 2010; Cawood et al., 2013; Condie and Kröner, 2013; Niu et al., 2013; Gazel et al., 2015; Whattam and Stern, 2016; Hacker et al., 2015; Kelemen and Behn, 2016). However, there are several potential problems with the standard juvenile arc accretion model. First, island arcs alone are not able to explain the volume of crust generated in many accretionary orogens (Reymer and Schubert, 1986; Hawkesworth et al., 2009; Kemp et al., 2009; Scholl and von Huene, 2009; Stern and Scholl, 2010; Condie, 2013; Condie and Kröner, 2013). Second, most arc material is not solely composed of juvenile magmatic rocks sourced through melting and extraction from the mantle, but includes some portion of melt derived through reworking of evolved crust that existed prior to development of the arc (Condie and Kröner, 2013). Third, when evaluated in detail, some argue there is a poor geochemical fit between juvenile arc crust and bulk continental crust (Condie and Kröner, 2013; Niu et al., 2013). Lastly, juvenile arcs may not be buoyant enough to avoid subduction during accretion to continental margins (Condie and Kröner, 2013).

An alternate model suggests that accretionary orogens grow through repeated cycles of arc accretion; slab rollback forming an extensional basin that separates fragments of the earlier arc; and basin closure due to increased convergence rate, shallow subduction, or collision of an arc/continental fragment or oceanic plateau (Collins, 2002; Cawood and Buchan, 2007; Kemp et al., 2009; Fig. 1). This "tectonic switching" model may explain the limited amount of more juvenile island arc material within accretionary orogens as accreted backarc basin sedimentary and igneous rocks are important orogen constituents. This model, too, suggests that rifting of preexisting arcs and/or the continental margin may provide a substrate for subsequent arcs, leading to more chemically evolved and buoyant arc complexes that are more easily preserved.

This field guide explores the geology in a portion of one of the largest preserved accretionary orogens—the Yavapai-Mazatzal provinces of the western United States (Fig. 2). These provinces (also termed the Colorado Province, e.g., Bickford et al., 1986) have been referred to as type sections for Proterozoic accretionary orogens (Reed et al., 1987; Bowring and Karlstrom, 1990; Karlstrom et al., 2004; Whitmeyer and Karlstrom, 2007). However, there remains no consensus over the competing hypotheses of formation as a result of accretion of juvenile magmatic arcs or alternative mechanisms such as tectonic switching. The northern Colorado Front Range is an excellent location to explore the geology of these provinces and consider the applicability of these models.

A similar field trip was planned for the 2013 Geological Society of America annual meeting (Mahan et al., 2013). However, catastrophic flooding in the Front Range in September of

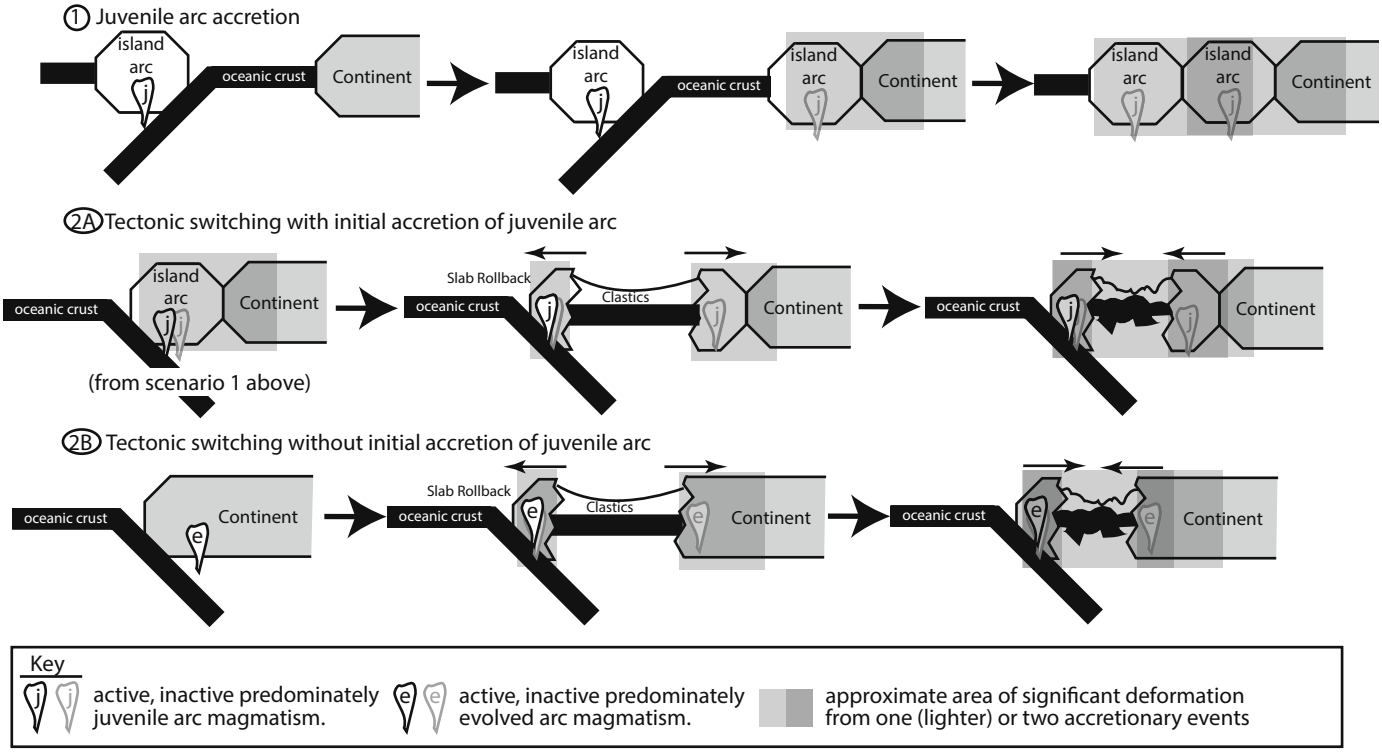

Figure 1. Generalized models for accretionary orogens; see text for details.

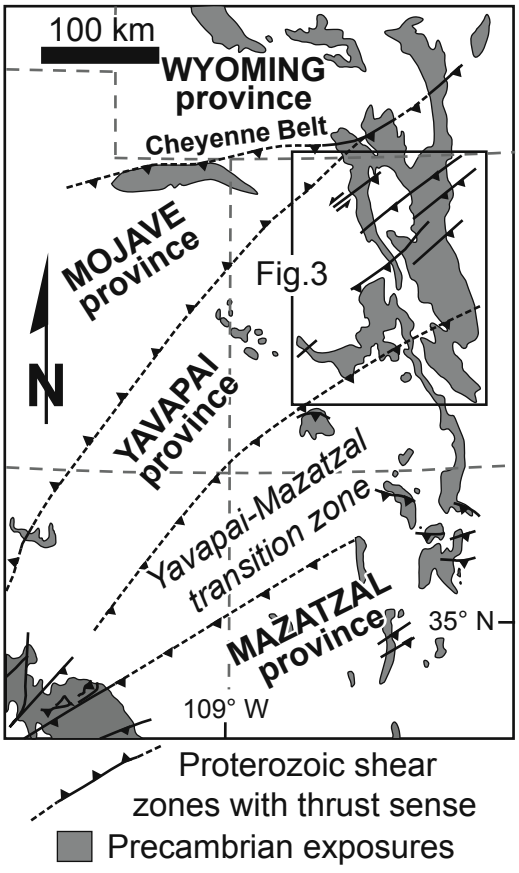

that year destroyed many canyon roads and thousands of homes and resulted in the loss of life. The field trip, therefore, could not be offered during that meeting, and river channel migration and road reconstruction drastically changed many of the guide's stops. This, in conjunction with a plethora of new data, means that this trip guide provides important updates and augments Mahan et al. (2013). Together, these guides provide a comprehensive overview of rock exposures, data sets, and ideas regarding the origin and tectonic evolution of these rocks.

PROTEROZOIC GEOLOGY OF THE NORTHERN COLORADO FRONT RANGE

The ca. 1.8–1.6 Ga Yavapai-Mazatzal provinces are portions of a great accretionary orogen that developed marginal to the supercontinent Nuna (Evans and Mitchell, 2011). Approximately 25% of North America may be underlain by these rocks. The subdivision of the Yavapai-Mazatzal provinces (Fig. 2) originally was based on whole rock Nd and Pb isotopic studies in the western United States (DePaolo, 1981; Nelson and DePaolo, 1985; Bennett and DePaolo, 1987; Reed et al., 1987; Aleinikoff et al., 1993a), and resulted in the identification of

Figure 2. Major Precambrian exposures and inferred Proterozoic provinces of the western United States (after Karlstrom and Williams, 2006).

a northern ca. 1.8–1.7 Ga juvenile arc belt and a southern ca. 1.7–1.6 Ga juvenile arc belt (Condie, 1982; Nelson and DePaolo, 1985; Aleinikoff et al., 1993a). These belts were later correlated with similar aged rocks in Arizona—the Yavapai and Mazatzal provinces (Fig. 2; Karlstrom and Bowring, 1988; Bowring and Karlstrom, 1990; Karlstrom and Daniel, 1993; Shaw and Karlstrom, 1999; Karlstrom et al., 2004). This field trip focuses on the evolution of the northern Colorado portions of the Yavapai province.

The northernmost part of the Yavapai province in the Rocky Mountains (Fig. 3) is the ca. 1.78 Ga Green Mountain arc (GMA), which was accreted to the margin of the Archean Wyoming Province along the Cheyenne belt (e.g., Karlstrom and Houston, 1984; Fig. 2) during the Medicine Bow orogeny (ca. 1.78–1.75 Ga;

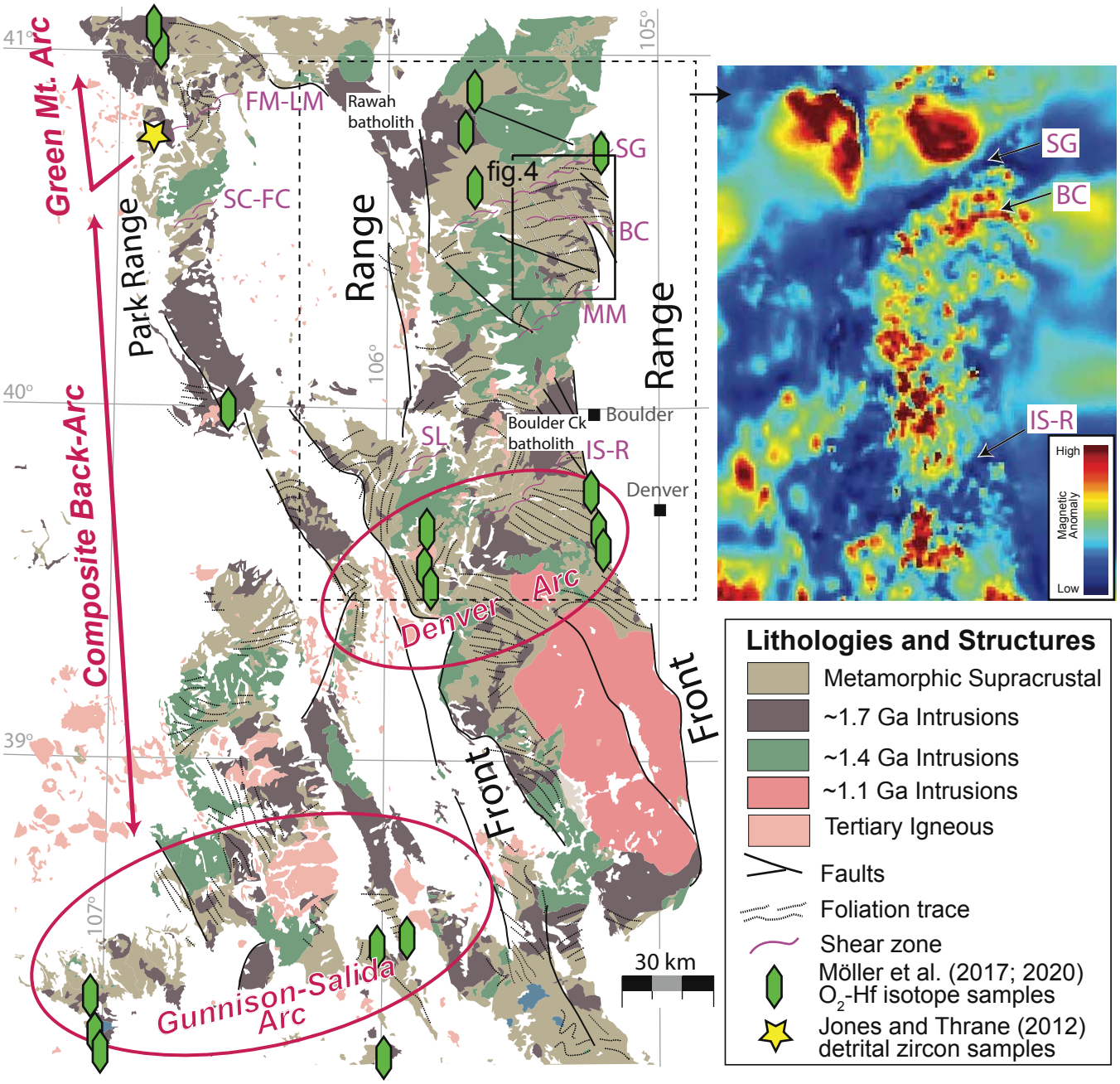

Figure 3. Major Proterozoic tectonic features of the Colorado Rocky Mountains. Shear zones are Farwell Mountain–Lester Mountain (FM-LM), Soda Creek–Fish Creek (SC-FC), St. Louis (SL), Skin Gulch (SG), Buckhorn Creek (BC), Moose Mountain (MM), and Idaho Springs–Ralston (IS-R). CK—Creek. Based on Tweto and Sims (1963), Tweto (1979), and Sims et al. (2001). (Inset) Magnetic anomaly map showing correlation between major shear zones and distinct magnetic signatures (Bankey et al., 2002).

Chamberlain, 1998; Jones et al., 2010, 2011). The GMA is composed of metamorphosed bi-modal igneous rocks and has been interpreted to represent either an island arc or a continental arc (Jones et al., 2010, 2011). The southern exposed limit of the GMA is typically defined by the Farwell Mountain–Lester Mountain shear zone and its inferred extension to the northeast (Fig. 3; Tyson et al., 2002). South of the Farwell Mountain-Lester Mountain shear zone is a region dominated by metamorphosed clastic sediments and igneous arc rocks. The origin of these rocks south of the GMA is controversial, but some interpret these rocks as the remnants of a backarc basin (e.g., Reed et al., 1987; Premo et al., 2010b; Jones et al., 2010)—termed the Composite back-arc (Fig. 3; Reed et al., 1987). Within the Composite back-arc, other arc components that collided with the GMA may exist such as the ca. 1720 Ma Rawah batholith (Premo and Van Schmus, 1989; Tyson et al., 2002). DeWitt et al. (2010) and Premo et al. (2010b) proposed that a second arc exists west of Denver (Fig. 3), the Denver arc, with the region between the GMA and Denver arc identified as the Poudre Basin. Remnants of the Poudre Basin may extend west to at least the Park Range (see below).

South of the Composite back-arc, ca. 1.78–1.73 Ga magmatic rocks with arc affinities have been described and are referred to as the Gunnison-Salida arc (e.g., Reed et al., 1987; Moscati et al., 2017; Fig. 3). These rocks are argued to be either juvenile or evolved (cf. Bickford et al., 2008; Karlstrom et al., 2007), with debate over whether they represent a separate, independent arc (e.g., Premo et al., 2010b), or if they are a rifted GMA fragment (Moscati et al., 2017), similar to the Denver arc.

Much of the debate regarding which tectonic model is most applicable to Colorado's Paleoproterozoic crust in part balances on how data from these rocks are best interpreted. Some argue that the data indicate that much of the region is underlain by extended evolved Archean and Trans-Hudson orogen rocks (e.g., Hill and Bickford, 2001; Bickford and Hill, 2007). If true, the tectonic switching model provides mechanisms to explain the presence of older crust (Fig. 1, scenario 2B). But the tectonic switching model does not require the presence of older crust if it is preceded by juvenile arc accretion (Fig. 1, scenario 2A). Regardless, many models for Proterozoic tectonics and crust formation in northern Colorado invoke some variation of tectonic switching (e.g., Condie, 1982; Cavosie and Selverstone, 2003; Dewitt et al., 2010; Jones et al., 2010; Premo et al., 2010b). However, others argue that little evidence exists for widespread evolved crust and favor the juvenile arc accretion model (e.g., Karlstrom et al., 2007; Fig. 1, scenario 1).

The extent of juvenile Paleoproterozoic crust in Colorado was recently tested by Möller et al. (2017, 2020) using combined Hf and O isotopic analysis of zircons from magmatic rocks with well-constrained ages and whole rock Nd isotopes (Fig. 3; Premo et al., 2010a, 2010b; Tables S1–S3; methods in Supplemental Material[1]). The study focused on the oldest rocks in the GMA, the Denver arc, and the Gunnison-Salida arc. Most samples show little evidence for inherited cores and limited scatter in mantle-like $\delta^{18}O$ values (4.3–6.6 ‰), typical of juvenile crustal provinces. No age-$\delta^{18}O$ correlation is observed, indicating crustal input did not increase into magma sources over time. Some of the Gunnison-Salida arc samples show oxygen-Hf trends consistent with higher crustal input, but most only show mantle-like values. Based on this limited data set, the three studied regions do not show distinct isotopic differences in Nd-Hf, and Nd-$\delta^{18}O$ data are near mantle values. Therefore, this work helps confirm earlier isotopic studies that Colorado's crust is juvenile.

Though confirming that Colorado's crust is juvenile is important, distinguishing the juvenile arc accretion model from the tectonic switching model when only juvenile crust is involved remains problematic (Fig. 1, scenario 1 versus 2A). Therefore, additional work is needed to test the applicability of these models. This guide details geochemistry and geochronology data from the field-trip area, which has only previously been presented in conference abstracts (e.g., Dewitt et al., 2010; Chumley et al., 2017; Hooker et al., 2019; Baird et al., 2019; now available in Tables S4–S6 [see footnote 1]) that helps constrain the tectonic history and setting of these rocks.

FIELD-TRIP AREA

This trip focuses on the origins, age, deformation, and metamorphism of the Paleoproterozoic rocks in the area around and between the Big Thompson, Rist, and Poudre Canyons in the northern Colorado Front Range (Fig. 4). For more thorough rock descriptions, see Cole and Braddock (2009) and Workman et al. (2018) and references therein.

Lithologies

Poudre Canyon Granitic Gneiss

The oldest rock unit in the broader field-trip area is granitic gneiss found in the cores of antiforms along the Poudre Canyon (Fig. 4). Gneiss protoliths are interpreted to be variably plutonic to volcanic (Workman et al., 2018). A date of 1776 ± 7 Ma (sample EDW 8-31-08-2 of Table S2; all errors are at the 2σ level) from an exposure north of the Poudre Canyon mouth is interpreted as the age of the granitic gneiss protolith. This date is consistent with the age of the GMA, and DeWitt et al. (2010) suggests that this granitic gneiss is basement to the metasedimentary sequence.

Metasedimentary Rocks

Much of the field-trip area is underlain by metasedimentary rocks, now folded and metamorphosed into biotite schist and gneiss, quartz-feldspar schist, knotted schist, and porphyroblastic biotite schist (Fig. 4). These rocks were originally a series of turbidites thought to be sourced from granite- and quartzite-dominated terranes (Condie and Martell, 1983). Using a variety of bulk chemistry parameters, Lehman (2020) reports that the

[1]Supplemental Material. Methods and data. Please visit https://doi.org/10.1130/FLD.S.20493147 to access the supplemental material, and contact editing@geosociety.org with any questions.

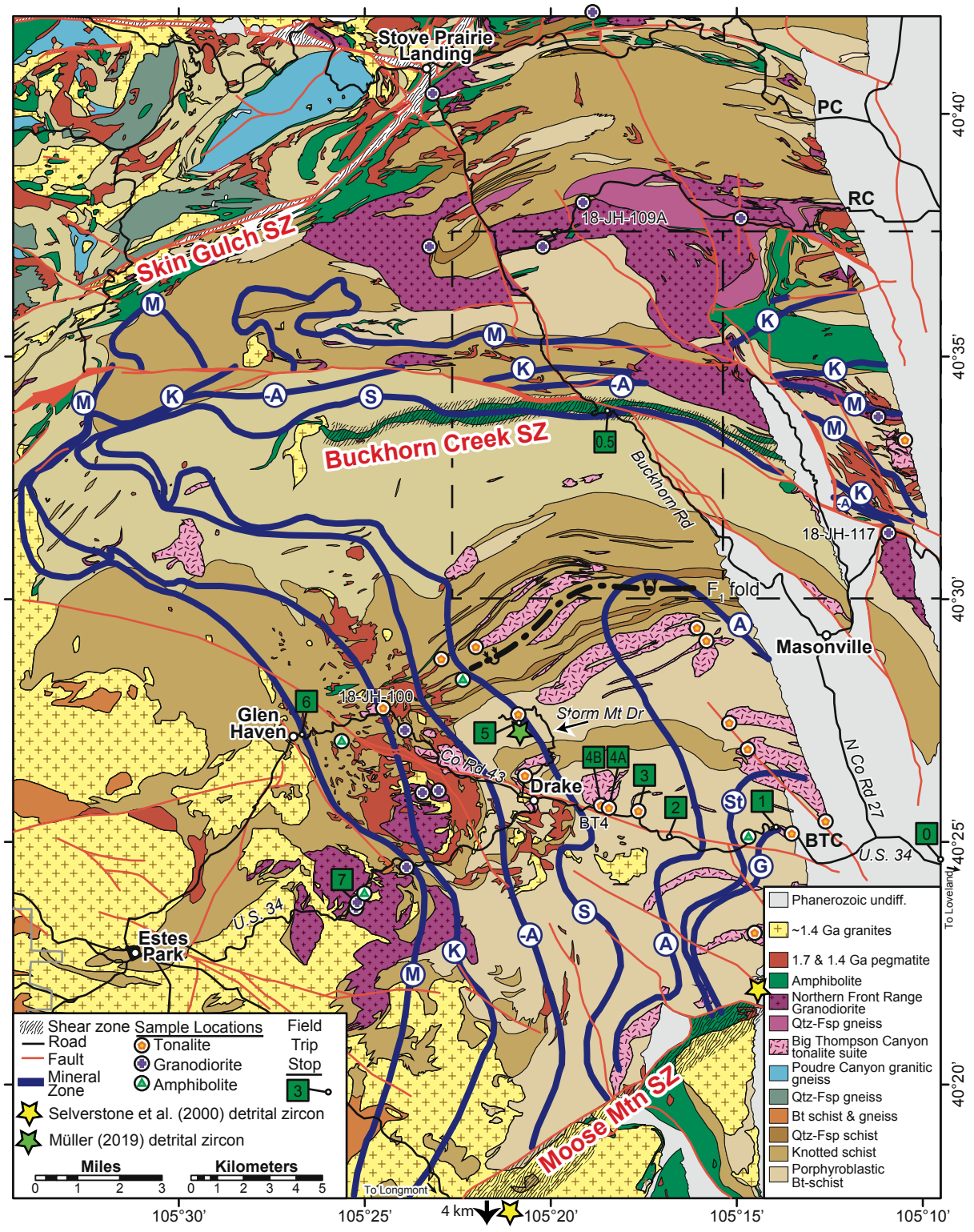

Figure 4. Geology of the northern Colorado Front Range (after Abbott, 1976; Shaver et al., 1988; Braddock et al., 1988a, 1988b, 1989a, 1989b; Nesse and Braddock, 1989; Cole and Braddock, 2009, and references therein). The field trip generally focuses on the area between the Moose Mountain and Skin Gulch shear zones. Metamorphic mineral zone boundaries with increasing grade: G—garnet-in; St—staurolite-in; A—andalusite-in; S—sillimanite-in; -A—andalusite-out; K—K-feldspar in; M—partial melt-in. Geochronology samples are labeled with a sample number. The mouths of the Poudre Canyon (PC), Rist Canyon (RC), and Big Thompson Canyons (BTC) are labeled. Bt—biotite; Fsp—feldspar; Qtz—quartz; SZ—shear zone. The left and right dashed boxes are the Buckhorn Mountain and Horsetooth Reservoir quadrangles, respectively.

metasediments are chemically similar to shale and graywacke, and discrimination diagrams suggest a continental island arc setting. In lower metamorphic grade areas, gradation between the meter to centimeter–scale quartz-rich (sandstone protolith) and mica-rich (mudstone protolith) layers can be identified locally and are interpreted as the relict graded beds of the turbidites (Mahan et al., 2013).

Figure 5 summarizes the published detrital zircon geochronology from this area and includes two samples from the Park Range to the west of the field-trip area (Fig. 3; Selverstone et al., 2000; Jones and Thrane, 2012; Müller, 2019). The two samples collected near the Moose Mountain shear zone (Fig. 4) have relatively few analyses and extensive Pb-loss; all the data for these samples are shown. A number of key observations can be made from these generally similar data sets. First, the collective range in maximum depositional age is ca. 1776–1739 Ma. Given that the region was tectonically active during sediment deposition, the maximum depositional age for each sample should reasonably approximate the age of deposition (Cawood et al., 2012). Next, the most prominent sediment source is generally attributed to the ca. 1780 Ma Green Mountain and/or Denver arcs (northern three samples; Jones and Thrane, 2012), though ca. 1840 Ma sediment is also variably important and is generally attributed to the Trans-Hudson orogen located in the Dakotas, or possibly closer in east-central Wyoming (Jones and Thrane, 2012; Worthington et al., 2016; Chamberlain and Mueller, 2019). Lastly, all samples have at least trace quantities of Archean zircon, which is likely sourced from the Wyoming Province (e.g., Selverstone et al., 2000; Jones and Thrane, 2012).

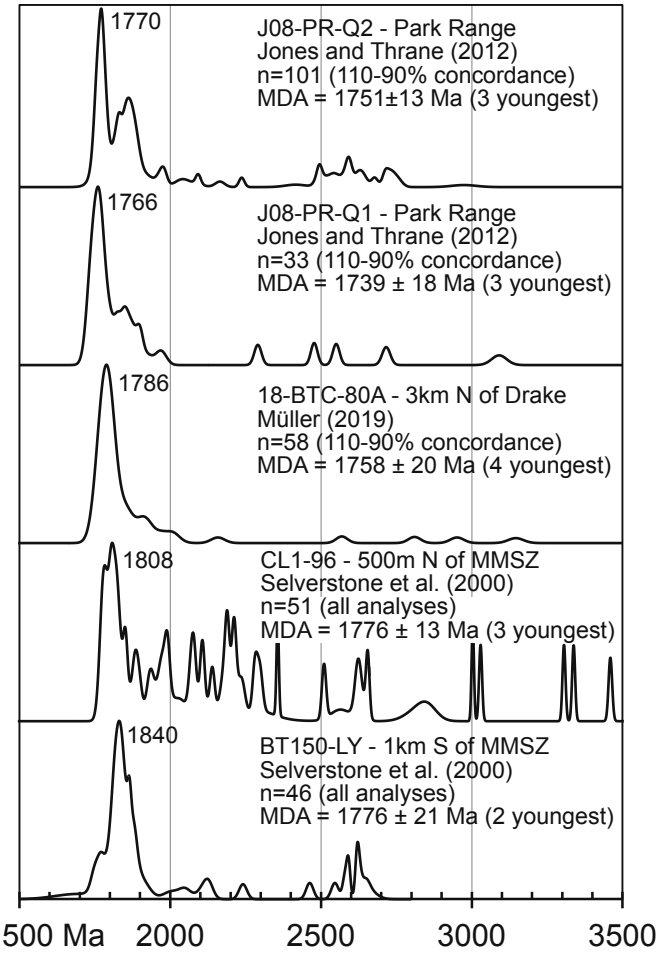

Figure 5. Summary age-probability diagrams for detrital zircon U-Pb age data from the inferred extent of the Poudre Basin, organized from north (top) to south (bottom). Age of the most prominent peak is shown. MDA—maximum deposition age estimation, in all cases only near-concordant analyses were considered; MMSZ—Moose Mountain shear zone.

Amphibolite

Deformed amphibolite commonly occurs as concordant or near concordant bodies within the metasedimentary sequence (Fig. 4; Braddock and Cole, 1979). One body north of the field-trip area near the Wyoming border has a reported protolith emplacement age of 1779 ± 5 Ma (Workman, 2008). Around Poudre Canyon, DeWitt et al. (2010) characterize the amphibolites as the remains of a mafic dike swarm.

As part of undergraduate research, A. Chumley obtained bulk rock geochemistry of seven amphibolite samples from the Big Thompson Canyon area (Table S4; Fig. 4; Methods in Supplemental Material). These samples are compared to amphibolite samples from the Buckhorn Creek shear zone published by Cavosie and Selverstone (2003). All amphibolites are tholeiitic with the Big Thompson Canyon samples possessing a moderately sloping rare-earth element (REE) profile with, on average, a minor negative Eu anomaly (Fig. 6). A multielement diagram shows that the amphibolites are enriched relative to normal mid-ocean ridge basalt. Compared to the REE trend, the amphibolites have distinct depletion in Nb and Zr, variable depletion in Ti and P, and generally enrichment in K, Pb, and Sr.

Cavosie and Selverstone (2003) concluded that the amphibolite body exposed along the Buckhorn Creek shear zone represents a slice of seafloor and it is chemically distinct from other amphibolite bodies in the area. Although data from other amphibolite bodies are limited, the comparison here does not suggest the Buckhorn Creek shear zone body is chemically distinct. Whereas the strong tholeiitic signature of all the samples is consistent with a mid-ocean ridge origin, the depletion of Nb, Zr, and Ti, with enrichment of K, Pb, and perhaps Sr suggests the magma that produced the amphibolite protolith was influenced by a subduction zone.

Big Thompson Canyon Tonalite Suite

Tonalitic rocks (Fig. 4), termed the Big Thompson Canyon tonalite suite (BTCt), are typically fine- to medium-grained, massive to foliated and lineated plagioclase-quartz-dominated rocks. Biotite and alkali feldspar are common, although the latter has a mode typically less than 10%, which indicates the rocks are generally true tonalites. Muscovite is also found in some outcrops. BTCt bodies vary in size but are generally sill-like and

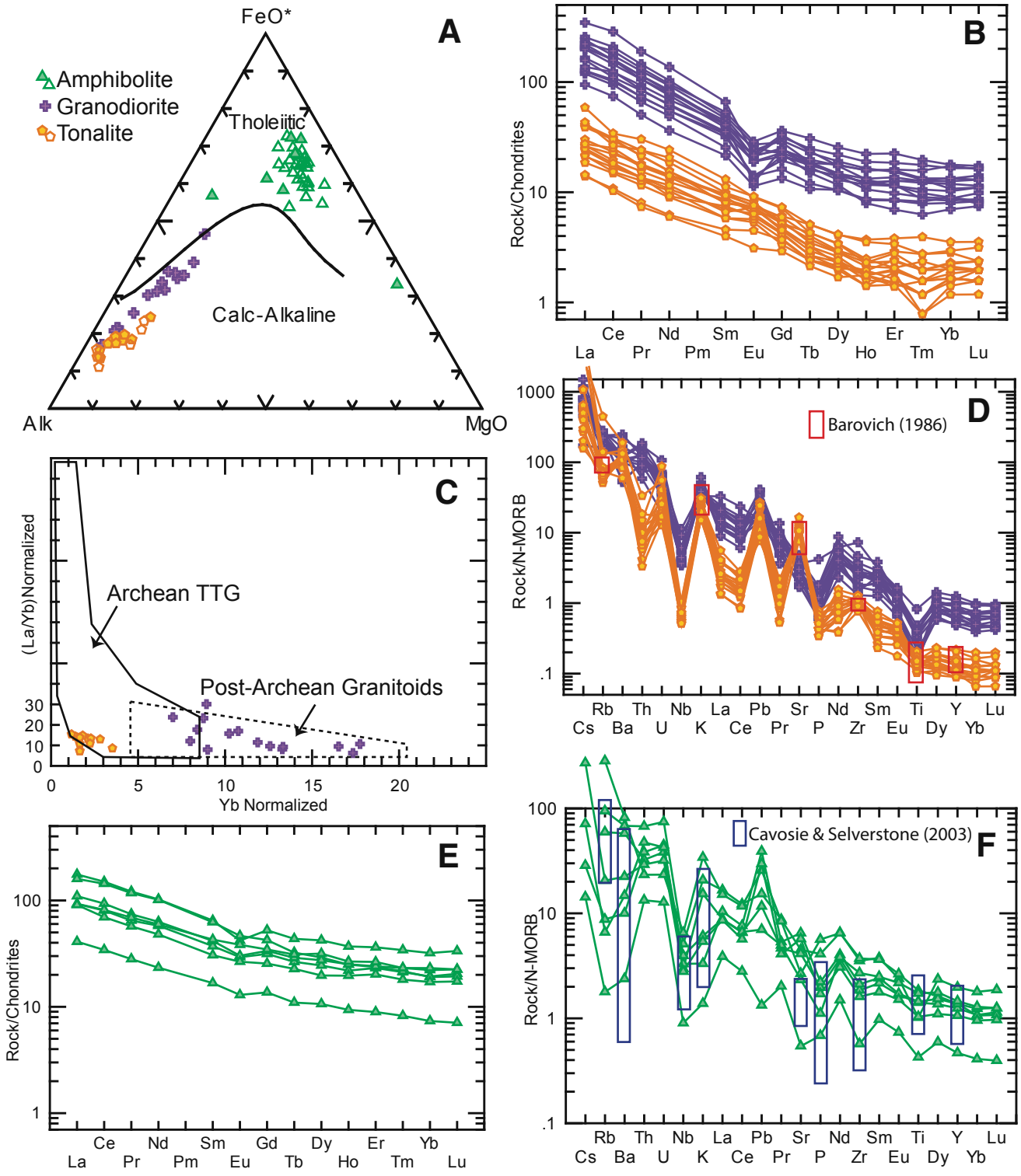

Figure 6. Bulk rock geochemistry of igneous and metaigneous rocks discussed. Symbol key for all diagrams is shown in A. Unfilled amphibolite symbols are data from Cavosie and Selverstone (2003), unfilled tonalite symbols are data from Barovich (1986), and all other data are presented in Table S4 (see text footnote 1). (A) Alk-FeO*-MgO (AFM) diagram (Alk = K_2O+Na_2O; F = all Fe as FeO; M = MgO; Irvine and Baragar, 1971). (B) Chondrite normalized rare-earth element diagram for the granitoids (Sun and McDonough, 1989). (C) Normalized La/Yb vs Yb diagram for the granitoids (Martin, 1993). TTG—tonalite-trondhjemite-granodiorite. (D) Normal mid-ocean ridge basalt (N-MORB) normalized multielement diagram for the granitoids (Sun and McDonough, 1989). (E) Chondrite normalized rare-earth element diagram for the amphibolites (Sun and McDonough, 1989). (F) Normal mid-ocean ridge basalt (N-MORB) normalized multielement diagram for the amphibolites (Sun and McDonough, 1989).

are predominantly found north of, south of, and along the Big Thompson Canyon between the canyon's mouth and the town of Drake. The BTCt has calc-alkaline chemistry; lacks or has a slightly positive Eu anomaly; and has distinct enrichment in U, K, Pb, and Sr and depletion in Nb, Ti, Dy, Y, Yb, and Lu (Chumley et al., 2017; Hooker et al., 2019; Table S4; Fig. 6). The BTCt has chemistry consistent with adakite or tonalite-trondhjemite-granodiorite (TTG) suites based on a number of criteria including normalized La-Yb concentration (Fig. 6C). A lack of a negative Eu anomaly and low heavy REEs is also common for adakites/TTGs and indicates the magma was sourced from the partial melting of an eclogite (Figs. 6B and 6D; Chumley et al., 2017; Hooker et al., 2019). Adakites or TTGs are generally interpreted to form from the partial melting of underplated mafic rocks or of subducted oceanic crust/plateau (e.g., Martin, 1999; Condie, 2005; Whattam and Stern, 2016; Johnson et al., 2017).

Barovich (1986) was the first to attempt to constrain the timing of BTCt emplacement. She obtained a multi-grain zircon U-Pb date of 1726 ± 15 Ma using isotope dilution-thermal ionization mass spectrometry (ID-TIMS) techniques. More recent work as part of undergraduate research by Hooker et al. (2019; Table S5; Fig. 7; Methods in Supplemental Material) using laser ablation-inductively coupled plasma-mass spectroscopy (LA-ICP-MS) demonstrates that zircon inheritance and Pb loss are significant issues. Therefore, the youngest, most concordant, and overlapping analyses from two samples were used to determine an emplacement age of 1742 ± 15 Ma. W. Premo dated zircon by U-Pb in four BTCt bodies with sensitive high-resolution ion microprobe-reverse geometry (SHRIMP–RG) and provided access to this data (Table S6; Methods in Supplemental Material). The collective weighted mean date of the SHRIMP-RG data is 1734 ± 8 Ma. Currently, the best estimate of BTCt emplacement

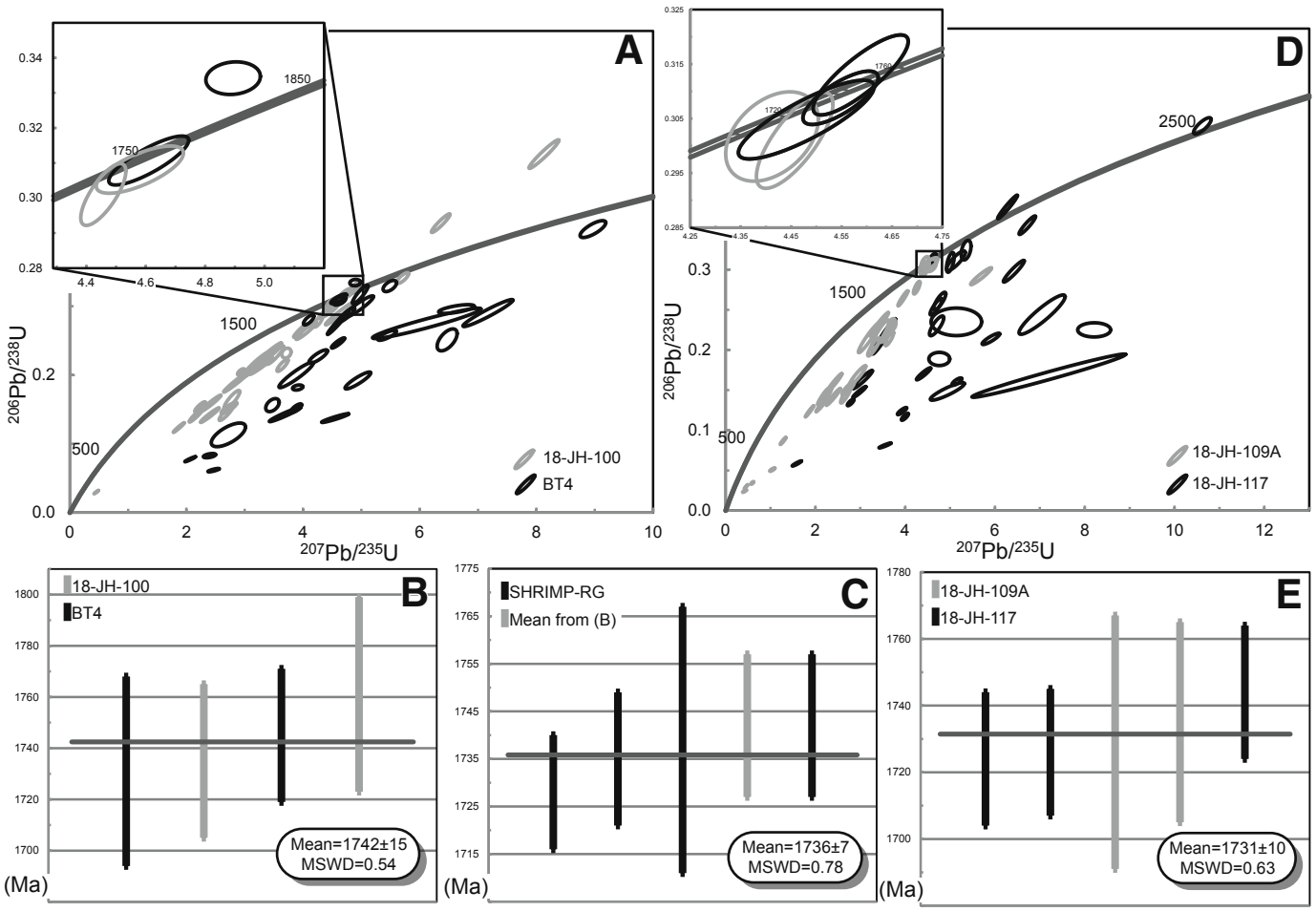

Figure 7. Tonalite and granodiorite U-Pb zircon geochronology data presented by Hooker et al. (2019; Table S5 [see footnote 1]). (A) U-Pb concordia diagram for all analyses from two Big Thompson Canyon tonalite suite samples. (Inset) U-Pb concordia diagram from the four youngest analyses with the most overlap in $^{207}Pb/^{206}Pb$ dates. (B) Weighted mean of the four analyses shown in the inset of A. MSWD—mean square of weighted deviates. (C) Weighted mean of four Big Thompson Canyon tonalite dates obtained by SHRIMP-RG (sensitive high-resolution ion microprobe-reverse geometry) (Table S6) and the date obtained in B. (D) Concordia diagram for all analyses from two granodiorite samples. (Inset) Concordia diagram from the five youngest analyses with the most overlap in $^{207}Pb/^{206}Pb$ dates. (E) Weighted mean of the five analyses shown in the inset of D.

age is considered to be a weighted mean $^{207}Pb/^{206}Pb$ date of 1736 ± 7 Ma, obtained by combining the data from the LA-ICP-MS and SHRIMP–RG techniques.

Northern Front Range Granodiorite

Granodioritic rocks found in the field-trip area (Fig. 4) are typically medium-grained, weakly to moderately foliated granodiorites to granites and occur as large irregular bodies mostly in the western Big Thompson Canyon and around Rist and Poudre Canyons. These rocks are typically thought to be associated with the 1714 ± 5 Ma (Premo and Fanning, 2000) Boulder Creek batholith (e.g., Braddock et al., 1970; Gable, 1980; Bucknam and Braddock, 1989; Fig. 3). Whereas these rocks generally look similar across the Front Range, the northern Front Range examples only have biotite as the mafic phase, whereas hornblende is common in the Boulder Creek batholith (Gable, 1980). Geochemically, these northern granodiorites, like the Boulder Creek granodiorite, are calc-alkaline (Fig. 6A; Table S4). Multi-element patterns show, most notably (Figs. 6B and 6D), a clear negative Eu anomaly, depletion in Nb and Ti, with enrichment in K and Pb. Such patterns are indicative of a subduction zone origin (Sun and McDonough, 1989; Chumley et al., 2017; Hooker et al., 2019).

Hooker et al. (2019) also dated two granodiorite outcrops northeast of Masonville and in Rist Canyon (Fig. 4; Table S5). The zircons in these samples have similar inheritance and Pb-loss issues that plagued the BTCt; so similarly, the most concordant, overlapping, and young analyses from the two samples were pooled to calculate a weighted mean $^{207}Pb/^{206}Pb$ date of 1731 ± 10 Ma (Fig. 7). This suggests these granodiorites are somewhat older than the Boulder Creek batholith and may not be directly related; hence they will be referred to as the northern Front Range granodiorites.

Silver Plume Granite

Although this guide focuses on the Paleoproterozoic history of the region, one Mesoproterozoic rock is important because it makes up a significant portion of exposures in the areas north, west, and south of the field-trip area. This rock is the ca. 1.45–1.35 Ga (Aleinikoff et al., 1993b) "A-type" or ferroan (e.g., Frost and Frost, 2011) granite and related rocks, often called the Silver Plume Granite (e.g., Anderson and Thomas, 1985; Anderson and Cullers, 1999). As will be discussed, intrusion of the Silver Plume granite may be associated with several deformation and metamorphic features observed on the trip.

Felsic Pegmatite and Aplite

Variably deformed dikes and sills of felsic pegmatite and related aplite are associated with the rock types discussed above. For all, alkali feldspar, quartz, and muscovite are nearly universally present. Other common minerals are plagioclase, tourmaline, and biotite; whereas garnet and beryl can be rare. As part of Master's research, Müller (2019) completed mineral separations on a few pegmatite bodies, but no zircon was obtained. Generally, it is believed that a generation of pegmatite is associated with each of the plutonic and metamorphic events that affected the region (Cole and Braddock, 2009; Workman et al., 2018).

Proterozoic Deformation

A number of major, mostly NE-trending shear zones transect the basement rocks of the northern Front Range (Figs. 2, 3, and 4). They are characterized by high-strain fabrics including mylonite and ultramylonite, and are commonly overprinted with Laramide-aged and possibly other brittle deformation (Tweto and Sims, 1963). Some of these shear zones appear to have originated at ca. 1.7 Ga, but have experienced reactivations at various times through to ca. 1.4 Ga and perhaps later (e.g., Shaw et al., 2001; Selverstone et al., 2000; Shaw et al., 2002; Cavosie and Selverstone, 2003).

The Skin Gulch shear zone is the southern limit of the ca. 1.78 Ga Poudre Canyon granitic gneisses (Workman et al., 2018). Deformation along the Skin Gulch shear zone is complex, but kinematic studies generally agree that southeast-side-up kinematics dominate (e.g., Solway, 2014). Monazite dates from the zone generally range from 1770 to 1720 Ma, but older ca. 1900 Ma and younger ca. 1400 Ma dates have also been reported (Hudson et al., 2004). The prominence of 1770–1720 Ma dates suggests that this is the time of deformation along the structure, but more work establishing the meaning of all dates is necessary.

The Buckhorn Creek shear zone has been proposed to have originated as an ocean transform that presently occurs along a ca. 1.7 Ga suture (Cavosie and Selverstone, 2003). Workman et al. (2018) contest this interpretation and some of the supporting field observations, thus concluding that no Proterozoic shear zone exists here.

The Moose Mountain shear zone is found predominately within the St. Vrain body of the 1.4 Ga Silver Plume granite (Fig. 3). Evidence suggests that north-directed, reverse-sensed shear along the zone was synchronous with granite intrusion (e.g., Selverstone et al., 2000; Workman et al., 2018). Debate exists regarding whether this ca. 1.4 Ga deformation is simply a result of pluton emplacement, or if it is evidence for regional convergent tectonism identified as either the Picuris (Daniel et al., 2013) or the Berthoud (Sims and Stein, 2003) orogeny. Selverstone et al. (2000) additionally argued for earlier, ca. 1.7 Ga, strike-slip motion along the zone. Differences in structural patterns and detrital zircon age spectra between the shear zone's adjoining rocks is used as evidence by Selverstone et al. (2000) to indicate that the structure juxtaposed blocks with different geologic histories. However, above we argue that no demonstrable difference in the detrital age spectra exists between the rocks that flank the structure.

Paleoproterozoic (meta-) igneous rocks between the shear zones show variable evidence for deformation, whereas the metasedimentary rocks are much more penetratively deformed. The most obvious structure associated with D_1 is a penetrative foliation sub-parallel to relict bedding, termed $S_{0/1}$ (Mahan et al.,

2013). Other D_1 structures include boudinage of quartz veins in the plane of $S_{0/1}$, tension gashes at a high angle to $S_{0/1}$, and folding of veins and gashes with axial planes sub-parallel to $S_{0/1}$. Reversals in younging direction as indicated by turbidite graded beds have been used to identify large-scale F_1 folds (e.g., Braddock, 1970; Fig. 3), but outcrop-scale F_1 folds affecting relict bedding can also be found (Mahan et al., 2013). Across the Big Thompson–Poudre Canyon areas, $S_{0/1}$ strikes in an arcuate pattern across the field-trip area: NW-SE in the northeast, E-W in the central area, and NE-SW in the west (Fig. 8). Contrary to the arguments that suggest the metasediments were unlithified during F_1 (Braddock, 1970; see also Cole and Braddock, 2009; Workman et al., 2018), aligned biotite parallel to $S_{0/1}$ (Mahan et al., 2013) and deformed coarse-grained granitic veins into F_1 folds (see Stop 3) strongly support that the metasediments were under at least greenschist facies conditions during D_1.

Identifying, distinguishing, spatially correlating, and establishing the relative timing of post-D_1 structures can be difficult. Quartz-rich layers may show no evidence of post-D_1 deformation, whereas mica-rich layers commonly, but not universally, display one or two post-D_1 crenulations. Cole and Braddock (2009) summarize for the region that F_2 folds/crenulations trend

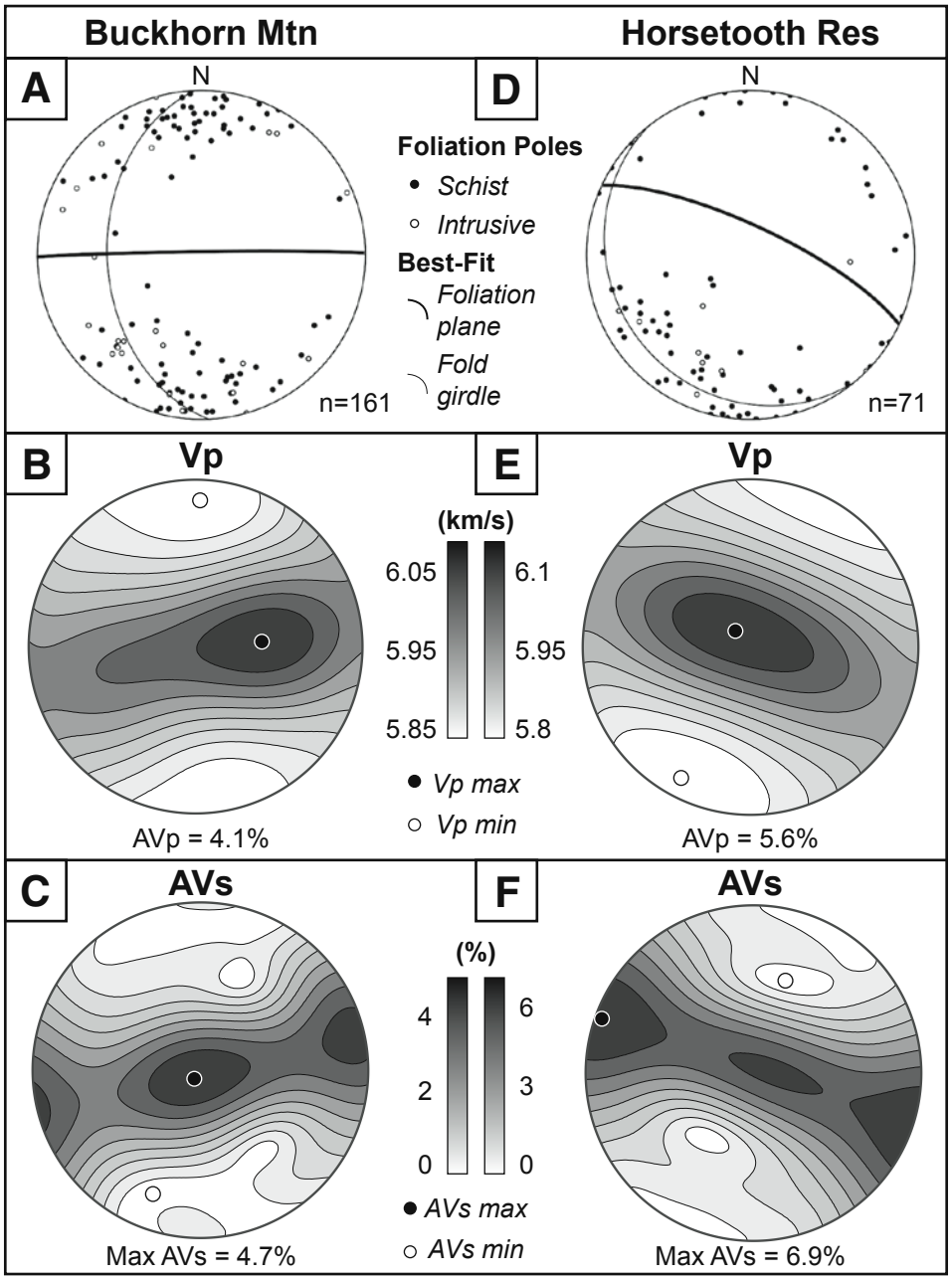

Figure 8. Equal-area lower hemisphere projections of structural and seismic properties calculated from geologic map data. (A) Foliations, best-fit foliations, and cylindrical fold girdles of input generalized schistose and intrusive crystalline rocks from the digitized geologic map of the Buckhorn Mountain quadrangle (Braddock et al., 1989a; Workman et al., 2018). (B) Calculated map-scale P-wave velocities (Vp) and P-wave anisotropy (AVp), as well as (C) S-wave anisotropy (AVs), based on structural data in A and input bulk elastic tensors (biotite gneiss, Erdman et al., 2013; isotropic granite, Frothingham et al., 2022). (D–F) Same as A–C, but from the Horsetooth Reservoir quadrangle (Braddock et al., 1989b).

to the E or NE. Barovich (1986) described a poorly developed S_2 fabric in the area east of Drake in the Big Thompson Canyon (Fig. 3), but we have not been able to identify this fabric. F_3 folds/crenulations trend to the N or NW (Braddock and Cole, 1979; Hutchinson and Braddock, 1987). Both F_2 and F_3 folds can have an axial planar foliation and these folds/crenulations may have developed at a similar time and constitute a conjugate set (Cole and Braddock, 2009). North of Drake, Mahan et al. (2013) identified two crenulations, both striking NW-SE that were identified as S_{3a} and S_{3b}. These designations will be used again here as it is unclear if other workers distinguished these structures and how they should be correlated regionally.

Geophysical Studies

Geophysical data can provide important insights into the crustal architecture. The CD-ROM (Continental Dynamics of the Rocky Mountains; Karlstrom et al., 2002; Tyson et al., 2002) experiment used geology and multiple seismic-imaging techniques to produce a north-south cross section from central Wyoming to central New Mexico. The cross section is just west of the Park Range, and multiple fossil subduction zones were proposed based on those studies. A north-dipping subduction zone is associated with the Farwell Mountain–Lester Mountain shear zone, whereas a south-dipping zone is associated with the Soda Creek–Fish Creek shear zone (Tyson et al., 2002).

The magnetic anomaly map of the northern Front Range (Fig. 3 inset) shows that some large batholiths create magnetic highs. The Skin Gulch and Idaho Springs–Ralston shear zones are associated with obvious low anomalies, suggesting they are of crustal scale. The Moose Mountain shear zone does not have an identifiable anomaly, but the amphibolite body associated with the Buckhorn Creek shear zone produces a positive anomaly.

Recent work by Frothingham et al. (2022) tested the vertical continuity of Colorado's crustal structure by comparing mapped surface features to their subsurface equivalents via receiver functions. P-wave to S-wave conversions contain characteristic flips in azimuthal polarity, where they occur across subsurface contrasts in dipping fabric anisotropy (e.g., Schulte-Pelkum and Mahan, 2014). These polarity flips spatially correlate with the strike of mapped surface structures (e.g., faults and foliations) across Colorado. These results, in tandem with the tendency for faults to be parallel to regional foliations (Fig. 4), suggest that Colorado's exposed surface features may be generally representative of the equivalent deep crustal structure. Furthermore, the uniquely oriented E-W–striking and NW-SE–striking micaceous foliation domains in the Buckhorn Mountain and Horsetooth Reservoir quadrangles, respectively (Braddock et al., 1989a, 1989b; Workman et al., 2018), lead to exceptionally strong seismic anisotropy (Fig. 8; Godfrey et al., 2000; Frothingham et al., 2022). Therefore, the unique seismic properties in this part of the northern Colorado Front Range may be ideal for future seismic experiments to further examine deep crustal geophysical correlations with surface features.

Metamorphism

The rocks in the field-trip area preserve a mappable sequence of metamorphic mineral zones that indicate an increase in metamorphic grade from east to west and from south to north (Fig. 4). With increasing grade, zones are delineated by garnet-in, staurolite-in, andalusite-in, sillimanite-in, andalusite-out, K-feldspar-in, and migmatite-in boundaries (Cole and Braddock, 2009). These rocks also locally contain cordierite at higher grades, but no cordierite-in boundary has been mapped.

Reported values for metamorphic pressure-temperature (*P-T*) conditions range from ~470 °C and 0.2 GPa for garnet zone rocks to >720 °C and 0.55 GPa for migmatite-zone rocks (Allaz et al., 2015). These *P-T* estimates are broadly consistent with those of most other workers (Nesse, 1984; Munn and Tracy, 1992; Munn et al., 1993; and Lehman, 2020) and delineate a metamorphic field gradient that falls below the aluminosilicate triple point. However, Selverstone et al. (1995, 1997) calculated maximum metamorphic pressures of 0.8–1.0 GPa based on garnet zoning and the composition of plagioclase inclusions in garnet. These pressures suggest that the *P-T* path followed by these rocks passed through the kyanite stability field. To our knowledge, there are no reported occurrences of kyanite in rocks from the northern Colorado Front Range (e.g., Nesse, 1984), so evidence for high-pressure metamorphism is generally contested (e.g., Workman et al., 2018).

Timing of Deformation and Metamorphism

Relative timing of deformation and metamorphism can be assessed via cross-cutting relations between deformation fabrics and porphyroblasts. Inclusion trails parallel to the S_1 foliation are found in porphyroblasts of garnet, staurolite, and andalusite. Sillimanite needles are often intergrown with fabric-forming biotite crystals and knots of sillimanite are commonly found in the foliation plane. In migmatite-zone samples, sillimanite may be folded along with biotite in the hinges of crenulation folds. These textural relationships suggest that porphyroblast growth was syn- to post-tectonic.

Multiple minerals may be retrogressed into pseudomorphs. Polycrystalline biotite within undeformed dodecahedrons or other similar shapes are locally common and indicate the prior existence of garnet. Accompanying these pseudomorphs, relict garnet can also be present. Undeformed pseudomorphs of an early generation of staurolite are also common, now often consisting of intergrowths of randomly oriented, fine-grained muscovite and chlorite. The pseudomorphs locally contain idiomorphic staurolite interpreted to be a second generation of growth (Shaw et al., 1999). These observations suggest that the pseudomorph-forming event, and the growth of a second generation of staurolite, were not accompanied by a phase of deformation. Similarly, we also have observed fresh garnet within other retrograded porphyroblast pseudomorphs (see Stop 3). Debate continues as to whether these collective porphyroblastic metamorphic features

can be generated by a single metamorphic cycle, or if multiple cycles occurred (e.g., Cole, 2004; Mahan et al., 2013).

Absolute timing of deformation can be constrained by considering the relative timing of deformation to rocks and minerals with geochronologic constraints. The ca. 1735 Ma BTCt intruded before or during D_1 (Mahan et al., 2013; see below) and the rocks were undergoing metamorphism at this time. Additionally, Müller (2019) obtained monazite geochronology data from a "knotted" sillimanite-andalusite-muscovite-biotite-quartz schist collected north of Drake (Stop 5). Thin sections from this rock display the $S_{0/1}$ fabric strongly and S_{3a} only weakly (Fig. 9). Monazite grains are preferentially aligned to $S_{0/1}$ and display a chemically mottled core and homogenous rims, which are also preferentially aligned to $S_{0/1}$ (Fig. 9). The monazite was dated using an electron microprobe and the U-Th-Pb_{total} technique (e.g., Allaz et al., 2020). The mean date of cores and rims were indistinguishable and collectively averaged 1723 ± 4 Ma, which is interpreted as the age of D_1 and accompanying metamorphism (Müller, 2019).

Ettsen (2022), as part of Master's research, similarly analyzed monazite via an electron microprobe from five migmatite-zone samples from Estes Park to north of Poudre Canyon. Three of the five samples contain monazite crystals aligned with S_1, and monazite cores range between 1730 Ma and 1700 Ma with a cluster around 1725 Ma, interpreted as the timing of partial melting and deformation, consistent with Müller's (2019) results. However, younger domains also exist. Four samples have slightly higher REE domains that lack shape-preferred orientation and provide dates that span 1700–1675 Ma, which Ettsen (2022) interprets to indicate that metamorphism outlasted deformation. Narrow rims found on monazite of two of these samples also recorded new monazite growth at ca. 1.4 Ga. One last sample studied near Estes Park is almost completely surrounded by ca. 1.4 Ga Silver Plume granite. Nearly all monazite domains here yield dates between ca. 1450 Ma and1400 Ma with the remaining domains providing dates between 1700 Ma and 1675 Ma. These data suggest that although the monazite in this sample might have recorded the Paleoproterozoic deformation and melting events, most of the monazite has overgrowths or has been thoroughly recrystallized by the thermal pulse associated with the intrusion of the Silver Plume granite.

Additional monazite electron microprobe U-Th-Pb_{total} data is provided by Shah and Bell (2012) for an area north of Drake. Most of their dates range from ca. 1885 Ma to 1600 Ma, suggesting prolonged or multiple monazite growths during this time, but some dates were probably from detrital grains. A second group of dates from ca. 1489 Ma to 1338 Ma (see also Lehman, 2020) indicates another period of growth during intrusion of the Silver Plume granite and/or the Picuris orogeny.

Evidence for multiple thermal pulses occurring after ca. 1700 Ma tectonism also comes from ^{40}Ar-^{39}Ar thermochronology of biotite, muscovite, and hornblende from within the Big Thompson Canyon (Shaw et al., 1999). The micas, with an Ar closure temperature of ~300–450 °C, consistently provide cooling dates of ca. 1400–1340 Ma. More importantly, hornblende, with a closure temperature of ~500–550 °C, provides a range of dates from 1600 to 1390 Ma. Modeling of these results by Shaw et al. (1999) suggests a discrete, short-lived thermal event reaching ~550 °C at ca. 1400 Ma associated with Silver Plume granite intrusion. The thermal pulse is regionally extensive and rocks far from Silver Plume granite bodies also show the resetting of ^{40}Ar-^{39}Ar dates.

The collective data above constrain fairly well that D_1 started as early as ca. 1735 Ma and may have ended by ca. 1720 Ma. The age of younger deformation events is unclear and some or all may have immediately followed D_1, or they could be related to the ca. 1.65–1.63 Ga Mazatzal orogeny (Duebendorfer et al., 2015), ca. 1.62–1.59 Ga deformation identified along the Cheyenne belt northeast of the Park Range (Duebendorfer et al., 2006), and/or the ca. 1.4 Ga Picuris orogeny (Daniel et al., 2013). Metamorphism was synchronous with and outlasted D_1, and at least locally, additional metamorphism can be attributed to Silver Plume granite intrusion.

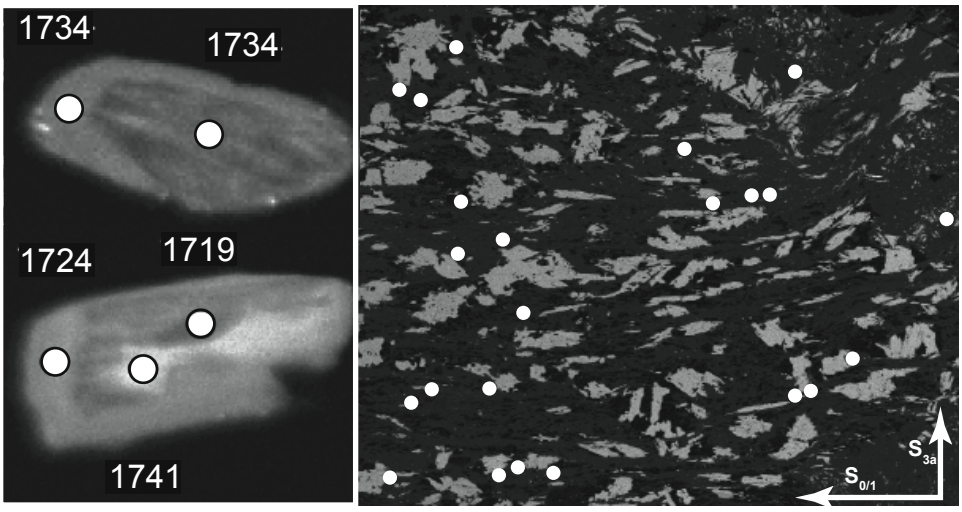

Figure 9. (Left) Two monazite grain Th X-ray maps and spot dates as determined by the electron microprobe U-Th-Pb_{total} technique. (Right) Mg X-ray map of a "knotted" sillimanite-andalusite-muscovite-biotite-quartz schist; biotite appears as gray. White dots mark the location of monazite grains as identified by a Ce X-ray map (not shown). Orientation of $S_{0/1}$ and S_{3a} in the thin section indicated. Vertical scale is ~2 cm. After Müller (2019; used with permission).

ROAD LOG AND STOP DESCRIPTIONS

Table 1 contains the road log. Many of the stops are based on Mahan et al. (2013) and include updated location information and/or data. Four new stops are described as well.

Stop 0. Devil's Backbone Open Space Parking Lot (Mahan et al., 2013)

(UTM NAD83 Zone 13T 487070, 4473454; 40.4117°N, 105.1520°W)

The Devil's Backbone Open Space (Loveland, Colorado) remains a useful field-trip stop due to its vault toilets and outdoor classroom. On mornings of weekend days in non-winter months, the open space is very popular and the parking lot fills up quickly. Starting in 2022, there will be a parking fee and organized trips require a special use permit from Larimer County.

Stop 0.5. Amphibolite along the Buckhorn Creek Shear Zone

(UTM NAD83 Zone 13T 473915, 4490498; 40.5648°N, 105.3081°W)

From Devil's Backbone Open Space, drive west 2.3 miles (3.7 km) on U.S. 34 and turn right (north) on N County Rd. 27, which will turn into Buckhorn Road. Continue 5.2 miles (8.4 km) to a T-junction in Masonville, turn left (west) to continue on Buckhorn Road. After driving ~8.0 miles (12.9 km) along Buckhorn Road past Masonville, the road narrows and becomes quite curvy and new outcrops begin to line the road that were created during road reconstruction induced by the 2013 flood. At 8.8 miles (14.2 km) from Masonville, park on the south side of the road; this should be the northern apex of a road curve and meander in Buckhorn Creek. Here, the north side of the road is lined with an extensive outcrop.

This location is in the heart of the amphibolite body that spans the Buckhorn Creek shear zone as described by Cavosie and Selverstone (2003). Here, the rock typically is a very dark-blue to green fine-grained amphibolite with a strong fabric, but coarser-grained rock with a less strongly developed fabric exists toward the east ~50 m. The fabric is east-west–striking and dipping very steeply down to the south, lineation is down-dip. Fabric is enhanced by stretched quartz ± calcite ± epidote veins parallel to foliation. Pyrite is common, particularly on fracture surfaces. Close inspection of regions with strong fabric reveals that the fabric anastomoses somewhat around pods with slightly weaker fabrics. In some locations, a sub-horizontal crenulation is apparent and Cavosie and Selverstone (2003) report that locally an older fabric with a sub-horizontal lineation also exists. Deformed pillow basalts are also reported, but have not been identified in this outcrop. The geochemistry of this and other amphibolite bodies is discussed above. During metamorphism, amphibolite should be a rheologically strong lithology in comparison to the quartz-rich units that flank this body. Therefore, given the fabric strength and its anastomosing character, we argue that Cavosie and Selverstone (2003) are correct in their identification of the Buckhorn Creek shear zone.

Stop 1. Big Thompson Canyon Mouth (Mahan et al., 2013)

(UTM NAD83 Zone 13T 480608, 4474666; 40.4224°N, 105.2286°W)

Return to the junction of N County Rd. 27 and U.S. 34, turn right and head west for 2.7 miles (4.3 km). Following U.S. 34 road reconstruction, the large pull-off on the north side of the road no longer exists in this area. Ample pull-off space now exists on the south side of the road just west of the mile 83 road marker. However, turning into this pull-off requires cutting across the east-bound lane adjacent to a blind corner. For safety,

TABLE 1. CUMULATIVE ROAD LOG

	km	mi	Notes
Stop 0	0.0	0.0	Devil's Backbone Open Space
Stop 0.5	23.8	14.8	Amphibolite along the Buckhorn Creek shear zone
Stop 1	28.2	17.5	Big Thompson Canyon Mouth (parking may be difficult)
Stop 2	33.8	21.0	Viestenz-Smith Mountain Park (outcrop no longer accessible)
Stop 3	35.1	21.8	Horseshoe/Big Curve
Stop 4	N/A	N/A	Midway: May not be publicly accessible; replaced by Stops 4A and 4B
Stop 4A	37.0	23.0	Midway East
Stop 4B	37.7	23.4	Midway West
Lunch	39.4	24.5	Forks Park
Stop 5	45.5	28.3	Storm Mountain Drive
Stop 5.5	46.7	29.0	Hyatt Beryl Pegmatite and Mine
Stop 6	65.7	40.8	Glen Haven
Stop 7	87.1	54.1	Upper Big Thompson Canyon

N/A—not applicable.

it is *recommended* that the pull-off for this stop is accessed from the west. One possible way to do this is to continue east through the Narrows 1.6 miles (2.6 km) until the Colorado Cherry Company is reached, utilizing its parking lot to turn around and then back-tracking to Stop 1. Similarly, attempting to head west along U.S. 34 from this stop is *not recommended*. The Dam Store, just 0.7 miles (1.1 km) to the east, provides a convenient parking lot to turn around in to head west on U.S. 34. Table 1 does not reflect possible extra driving to safely access this stop.

Apart from the parking details change, the description of this stop in Mahan et al. (2013) remains accurate, and this location has some of the lowest-grade metasedimentary rocks in the area, displays evidence for $S_{0/1}$ and a cross-cutting crenulation (probably S_{3a}), and numerous and obvious very light-gray sills of the BTCt.

Stop 2. Viestenz-Smith Mountain Park (Mahan et al., 2013)
(UTM NAD83 Zone 13T 475907, 4474425;
40.4201°N, 105.2840°W)

In the 2013 flood, Viestenz-Smith Mountain Park was essentially destroyed, but it has since been completely rebuilt by the City of Loveland. The park remains a popular weekend destination when it is open April–October. Though the north side of the river is now public, off-trail travel is strictly prohibited; thus, outcrops discussed in Mahan et al. (2013) are essentially inaccessible. The park entrance is 3.5 miles (5.6 km) west of Stop 1 on U.S. 34.

Stop 3. Horseshoe/Big Curve (Mahan et al., 2013)
(UTM NAD83 Zone 13T 475112, 4475027;
40.4255°N, 105.2934°W)

During U.S. 34 reconstruction, the road was re-routed and is no longer adjacent to the outcrops of interest. Fortunately, a parking area near the outcrop was added during the re-routing that allows, with a short hike, relatively easy access to the outcrops. Updated directions from Viestenz-Smith Mountain Park including driving 0.8 mi (1.3 km) west on U.S. 34 from the Viestenz-Smith Mountain Park entrance to a parking lot driveway on the southwest side of the road. Once parked, hike ~250 m north (upstream) along the Big Thompson River until outcrops just before the apex of the river meander are reached.

The series of outcrops from here to the apex of the meander provide excellent examples of rock types and features found in the area. This includes interlayered quartz-rich and mica-rich metasedimentary rock with asymmetric gradations between the layers that are interpreted as overturned relict turbidities (Mahan et al., 2013). Also of note are folded D_1 tension gashes and crenulated alkali feldspar-quartz-muscovite pegmatite and aplite with comb and lit par lit textures. A number of foliated and lineated sills of the BTCt also exist. The metasediments contain a myriad of porphyroblasts of biotite, tourmaline, andalusite, garnet, and staurolite—the latter two are partially or completely retrogressed (see also Mahan et al., 2013). A few pseudomorphed porphyroblasts appear to contain fresh garnet (Fig. 10A), suggesting multiple generations of garnet including partially or completely retrogressed garnet, plus fresh garnet overgrowing pseudomorphs.

After the 2013 flood, the ground surface adjacent to the outcrops was lowered by upwards of a meter and new outcrop was revealed, prompting a more detailed analysis of the structures in the area. One newly identified feature is a coarse-grained granitic vein that has been folded and $S_{0/1}$ is axial planar (Fig. 10B). Such a pre-D_1 vein helps support evidence that D_1 did not occur prior to protolith lithification, as this vein could not form in this manner if the host material was not highly cohesive and under metamorphic conditions. This exposure unfortunately has been subsequently covered with fill.

Also newly identified are two distinct post-D_1 structures (Fig. 10C). The more obvious is decimeter-scale folding or a crenulation of $S_{0/1}$ with the axial planes or axial planar foliation striking on average 155°/335° with a steep dip either to the NE or the SW (Fig. 10D). The structural style and orientation of this structure is consistent with S_{3a} described above and in Mahan et al. (2013). S_{3a} is also penetrative within the BTCt sills found in the area, which helps constrain their relative timing (Fig. 10C; Braddock and Cole, 1979; Hutchinson and Braddock, 1987). However, evidence from Stops 4A, 4B, and 5 place tonalite emplacement pre- or syn-D_1.

Also present is a spaced crenulation with a variably present axial planar foliation that strikes ~290° and dips steeply to the north (Fig. 10D). This deformation feature is consistent with S_{3b} of Mahan et al. (2013) and is likely younger than S_{3a}. Identification of S_{3b} here expands the spatial extent of where it has been identified along Storm Mountain Drive (Stop 5).

At least three mineral lineations exist (Fig. 10D); locally tourmaline occurs in two different orientation on the same $S_{0/1}$ surface. Though not perfectly aligned, the tourmaline lineation may be associated with S_{3a} and S_{3b}. However, another locally developed biotite lineation found on a $S_{0/1}$ surface plunges toward the WSW, and suggests that other deformation events have affected these rocks beyond just those described above.

Stop 4. Midway (Mahan et al., 2013)—Split into Stop 4A and Stop 4B

At the time of writing, the Idlewild Dam pull-off located at Midway is under construction (UTM NAD83 Zone 13T 473450, 4475421; 40.4290°N, 105.3130°W). The dam was completely destroyed in the 2013 flood, and it is unknown when the reconstructed pull-off will be public again. The high rock face ~400 m to the east was blasted back some meters during road reconstruction such that the main features discussed in Mahan et al. (2013)—the F_1 fold, examples of boudinaged BTCt sills, polycrystalline tourmaline sill borders, and large porphyroblasts—no longer exist. Alternative locations of the same features are described in Stop 4A and Stop 4B below.

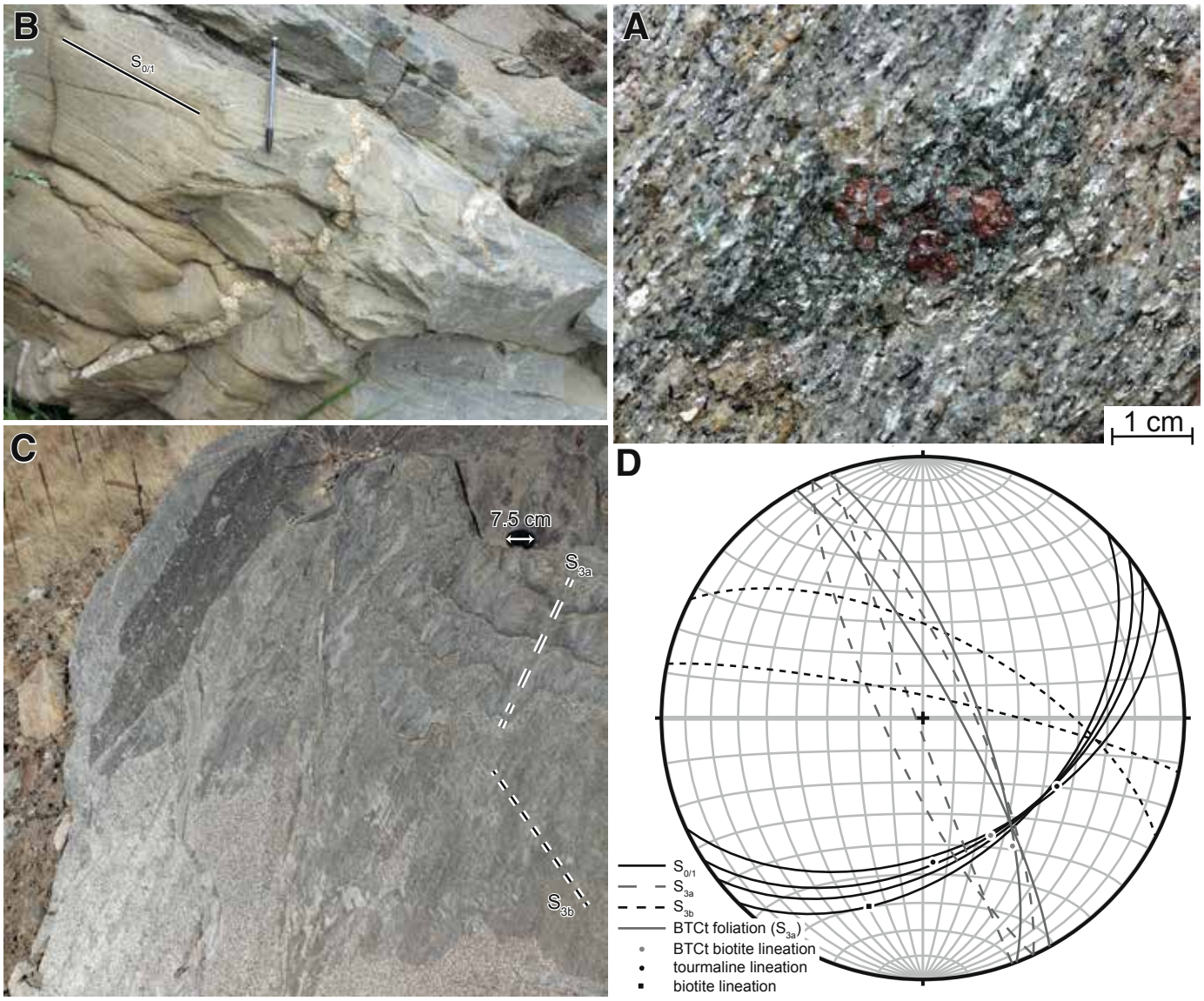

Figure 10. Newly identified features at Stop 3: Horseshoe Curve. (A) Muscovite-chlorite pseudomorph after staurolite (?) overgrown by fresh garnet. (B) Granitic vein with F_1 folds. (C) Outcrop surface is parallel to $S_{0/1}$ such that S_{3a} and S_{3b} are apparent. (D) Stereonet summarizing some of the structures at the stop location. BTCt—Big Thompson Canyon tonalite suite.

Stop 4A. Midway East
(UTM NAD83 Zone 13T 473849, 4475514;
40.4298°N, 105.3083°W)

Drive 1.0 miles (1.6 km) northwest on U.S. 34 from the Horseshoe Curve parking lot and park on the right (north) side of the road about in the middle of a new 300-m-long outcrop. There are two main features of interest here (Fig. 11). The first are a few outcrop surfaces parallel to $S_{0/1}$ that display a multitude of retrograded porphyroblasts that are ~1–30 cm in length. Though similar to exposures described in Mahan et al. (2013), these are not nearly as good of quality and fresh andalusite has not been identified. Also of interest are the multitude of BTCt sills in the area, many of which have been boudinaged in the plane of $S_{0/1}$.

Stop 4B. Midway West
(UTM NAD83 Zone 13T 473239, 4475521;
40.4299°N, 105.3155°W)

Drive 0.4 mile (0.6 km) west on U.S. 34 from Stop 4A and park on the right side (north side) of the road. This parking lot includes memorials for patrol officers and an engineer associated with the 1978 and the 2013 canyon floods, respectively.

Figure 11. Features of Stop 4A. (A) Dark retrograded porphyroblasts on $S_{0/1}$ surfaces. (B) Boudinaged Big Thompson Canyon tonalite suite sill (outlined).

At the east end of the parking area is a light-gray rock that is the edge of the Palisades stock of the BTCt. Hike southeast along the road ~75 m to an outcrop parallel to $S_{0/1}$ with dark "splotches" (Fig. 12). Be careful as you hike along U.S. 34; it is a *very busy road* so please stay as far off the pavement as possible. This outcrop has some notoriety regionally because it is quite striking. The splotches may be fairly round, elliptical, or blocky in shape and measure ~50 cm across. About a dozen are visible and they are biotite-rich with scattered muscovite. Internally the splotches have up to 1-cm-thick subvertical, often sigmoidal, quartzofeldspathic ± garnet veins. Additionally, a younger, generally millimeter-thick, similar set of veins trend down to the east. The splotches appear to be isolated from each other and are not part of a through-going biotite-rich sheet within the outcrop. The best interpretation is that the splotches are chocolate tablet structure (Ramsay and Huber, 1983) created by finite flattening strain in the plane of $S_{0/1}$. The blocky shape of some splotches, the two sets of cross-cutting veins—one of which can be sigmoidal—are all consistent with progressive variation in instantaneous maximum stretch direction that segmented a thin, competent, and once coherent biotite-rich layer. D_1, associated with BTCt boudinage (see below), likely generated the structure.

Above the face with the splotches is an irregularly shaped body of BTCt. This may be a large boudin; regardless, a BTCt apophysis is clearly boudinaged and is rimmed with polycrystalline tourmaline a few centimeters thick (Fig. 12A).

Hike another 150 m to the east along the road to a couple of prominent felsic pegmatite dikes. Dike mineralogy includes alkali feldspar, quartz, muscovite, tourmaline, garnet, and perhaps plagioclase. Locally, comb texture, zoning, and graphic texture are present. Cross-cutting relationships demonstrate that here the dikes are younger than the BTCt. No confirmed evidence that the pegmatites experienced D_1 can be found, but

some examples do contain S_{3a}. Though Mahan et al. (2013) suspected the pegmatites might be related to the BTCt, no good supporting evidence connecting these particular pegmatites to the BTCt exists. However, these pegmatites are mineralogically very similar to those discussed at Stop 5 and 5.5. See below for an expanded discussion regarding pegmatites of the area.

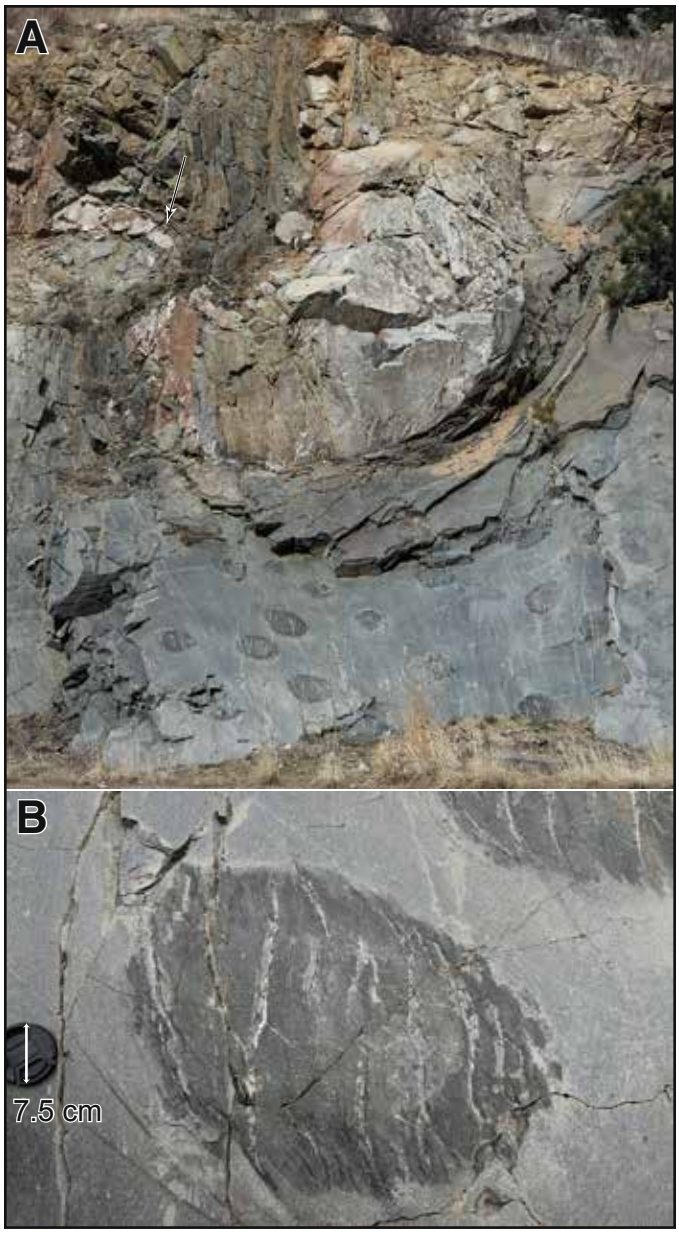

Figure 12. Some of the features of Stop 4B. (A) Irregular Big Thompson Canyon tonalite suite (BTCt) body is visible in the upper part of the photo. Arrow marks boudinaged BTCt apophysis rimmed by polycrystalline tourmaline. Lower part of the image is the black "splotches" exposure. (B) Photograph of the black "splotches" (chocolate tablet structure).

Lunch. Forks Park
(UTM NAD83 Zone 13T 471628, 4475849;
40.4328°N, 105.3345°W)

Forks Park is 1.1 miles (1.8 km) west of Stop 4B on the south side of U.S. 34. It is a small park with a vault toilet and Big Thompson River access. This is a great place to enjoy lunch and discuss geology.

Stop 5. Storm Mountain Drive (Mahan et al., 2013)
(UTM NAD83 Zone 13T 470537, 4478706;
40.4585°N, 105.3475°W)

Head west along U.S. 34 for 0.3 miles (0.5 km) from Forks Park, then turn right onto County Rd. 43. Then go another 0.3 miles (0.5 km) and turn right onto Storm Mountain Drive, which will eventually become a dirt road. Then turn left or keep left at the next three intersections to continue on Storm Mountain Drive: a T-junction after 2.2 miles (3.5 km), a Y-intersection after another 0.2 miles (320 m), and another Y-intersection after another 1.0 miles (1.6 km). A large pull-off on the left at 0.8 miles (1.3 km) after the last Y-intersection allows parking; however, this location is popular with campers, so other parking locations nearby may have to be utilized.

The petrographic description of this location and the analysis of the S_{3a} and S_{3b} deformation features are covered in Mahan et al. (2013). Additionally, zircon separated from a nearby outcrop proposed to contain relict overturned cross-bedding (Mahan et al., 2013) established that the metasediment protolith in this area was deposited ca. 1758 Ma (Fig. 5; Müller, 2019). Müller (2019) also obtained a monazite date of 1723 ± 4 Ma from a nearby outcrop that is argued to mark the timing of D_1 (see above).

The outcrops described in Mahan et al. (2013) and further analyzed by Müller (2019) require several hundred feet of off-trail hiking. This trip will focus on three fairly closely located outcrops. The first are the porphyroblastic mica-schist next to the vehicle parking. These outcrops display the $S_{0/1}$ and S_{3a} fabrics well; S_{3b} is also developed and can be easily identified with a bit of practice. Pseudomorphed cross-twinned staurolite is common. Andalusite is likely common, too, as it is present in great quantities at a number of nearby outcrops. Staurolite pseudomorphs are now dominated by very fine-grained muscovite and quartz ± chlorite ± biotite; mechanically this assemblage should be very weak. However, the S_{3a} crenulation deflect around the staurolite pseudomorphs, suggesting the porphyroblast existed before the development of S_{3a} (Fig. 13A). This relationship suggests that staurolite growth preceded S_{3a} development, whereas retrogression was subsequent to it.

From the tallest mica-schist outcrop, hike ~30 m south-southeast to another metasedimentary outcrop that is intruded by a 10-cm-thick pegmatite sill. This sill shows subtle pinch and swell consistent with stretch in the plane of $S_{0/1}$. Small offshoots at the end of the sill display both F_1 and F_{3a} folds (Müller, 2019). This is used as evidence that some of the pegmatite was

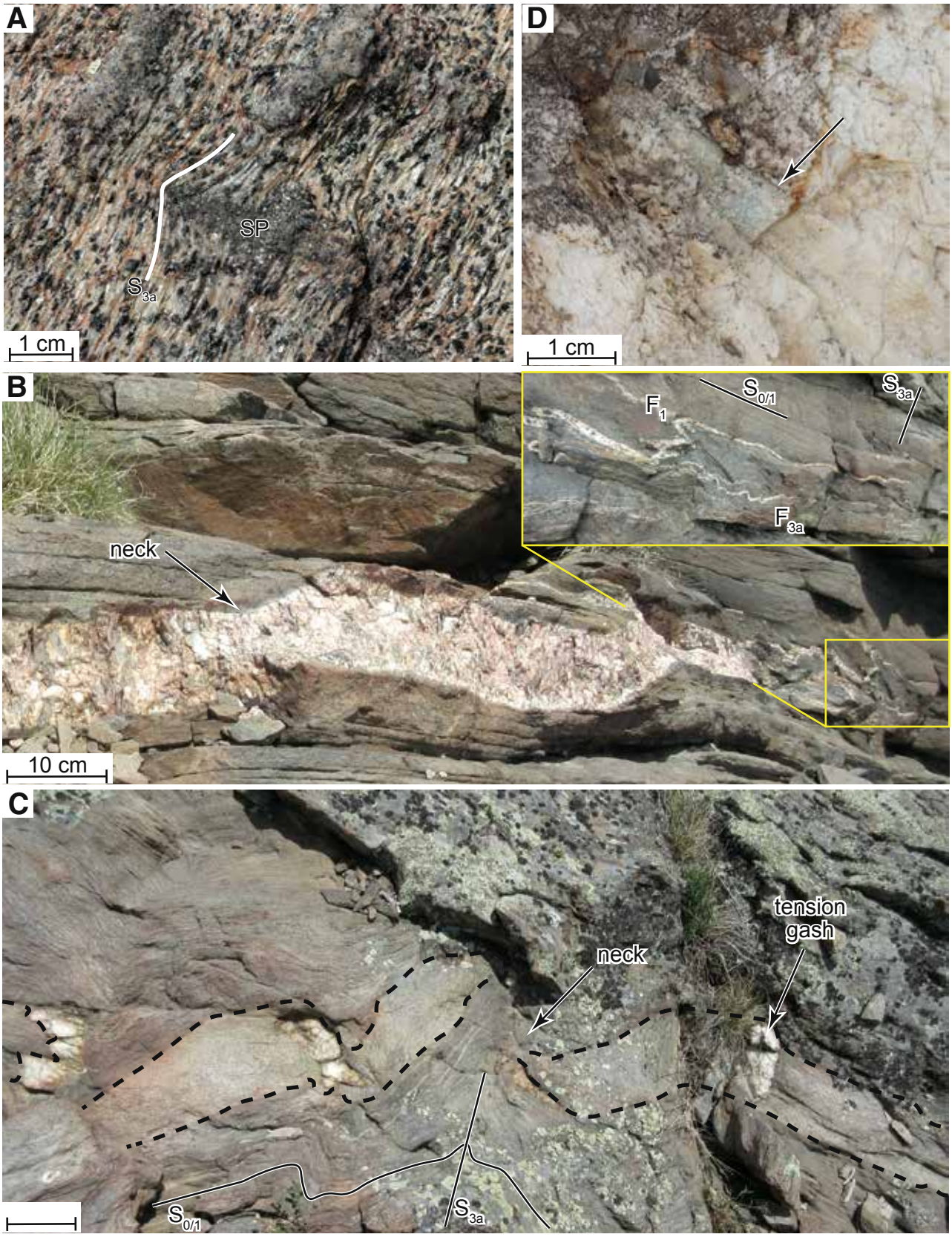

Figure 13. Features of Stop 5. (A) S_{3a} fabric wrapping around pseudomorphed staurolite (SP). (B) Comb-textured pegmatite sill displays pinch and swell. Inset: the terminus of the sill displays folding associated with the development of both $S_{0/1}$ and S_{3a}. (C) Sill of the Big Thompson Canyon tonalite suite is boudinaged (outlined) and filled with tension gashes formed during D_1; the boudins are in turn folded during D_{3a}. $S_{0/1}$ and S_{3a} are shown. (D) Small euhedral beryl (arrow) in pegamatite.

emplaced prior to the end of D_1 (Fig. 13B). Note that evidence for D_1 affecting the pegmatites of Stop 4B could not be found, and in general, evidence for D_1 affecting the pegmatites of this area is rarely observed. The BTCt shows evidence for D_1 at Stop 4A, which is similarly found ~500 m to the northwest of this location (Fig. 13C; Müller, 2019).

The third outcrop is one of the many pegmatite sills in the area. It is located ~50 m west-southwest of the deformed pegmatite sill outcrop, or ~50 m southwest of the tallest mica schist outcrop next to vehicle parking. This pegmatite is fairly representative of some of the larger pegmatites in the area and contains 30+-cm-long pink graphic perthites separated by white plagioclase. Comb-textured muscovite and tourmaline is also present and quartz pods and garnet are also locally found. Beryl is rare, but the west end of this exposure contains a few crystals (Fig. 13D). Here and at the Hyatt mine (Stop 5.5) there is obvious recent mineral-collecting activity targeting beryl, such that examples found by the authors have recently been removed or destroyed by attempted removal, so it is becoming increasingly difficult to find.

Stop 5.5. Hyatt Beryl Pegmatite and Mine
(UTM NAD83 Zone 13T 469731, 4478709;
40.4585°N, 105.3570°W)

Continue west on Storm Mountain Drive 0.7 miles (1.1 km) west of Stop 5 until an informal campground on the south side of the road is reached; park here. This, too, is a popular spot, so parking may be unavailable; if so, park just 0.1 miles (160 m) further west on Storm Mountain Drive at the apex of the next hairpin turn. From the informal campground, hike ~175 m east-northeast off the road to mining discard piles and the remains of a small mine pit. Property boundaries in the area are somewhat unclear. The southernmost discard piles should be U.S. Forest Service land, and the small mine pit appears to straddle the property boundary based on fence posts in the area. The main pit wall appears to be on private land.

The Hyatt pegmatite, located on the former Fred Hyatt ranch, is situated in the southern part of the extensive Crystal Mountain and Storm Mountain pegmatite field with >1300 pegmatites mapped and described (Thurston, 1955). The pegmatite was intermittently mined, primarily for beryl, starting after 1936 with peak activity in the 1950s (Gilkey, 1960; Thurston, 1955).

The Hyatt pegmatite is mostly located within a small BTCt stock (Braddock et al., 1970), though it does extend into the surrounding schist. A number of pegmatite bodies in the area are in contact with, or surround, BTCt bodies (Braddock et al., 1970; Bucknam and Braddock, 1989). The Hyatt pegmatite is >100 m diameter and is roughly concentrically zoned; it is one of ~30 that are concentrically zoned in the area. It has a discontinuous border zone, a fine-grained microcline-quartz-muscovite-beryl wall zone, a discontinuous and highly irregular quartz-albite-muscovite intermediate zone that contains beryl, and a coarse-grained microperthite core (Hanley et al., 1950). In many places where the granite pegmatite is in contact with the BTCt, the border zone is absent. However, where the pegmatite contacts schist, the border zone is well developed (Gilkey, 1960).

The microcline-quartz-muscovite-beryl wall zone makes up the bulk of the pegmatite and is composed of pink microcline, white to pink plagioclase, grayish quartz, and small books of muscovite, with minor quantities of light bluish-green to blue beryl that is uniformly distributed as euhedral crystals with an average size of 6 mm. The quartz-albite-muscovite intermediate zone is a series of disconnected lenticular pods between the wall zone and the core, chiefly composed of quartz, white albite, and greenish-white muscovite. Here, accessory beryl occurs as euhedral crystals and clusters with individual crystals reaching sizes as much as 0.3 m in diameter and up to 1.6 m in length. Also of note are local concentrations of black tourmaline, lithiophilite-triphylite, sicklerite-ferrisicklerite, purpurite-heterosite, uraninite, torbernite, autunite, bismuthinite, and pyrite (found in the triphylite). Lastly, the core is composed chiefly of white microperthite with minor milky quartz and black tourmaline (Hanley et al., 1950; Thurston, 1955).

Some of the early work on the Hyatt and related pegmatites was done by Margaret Fuller Boos, a pioneer of Front Range and pegmatite geology. In a time when geology was almost completely male-dominated, she was a highly productive field geologist and authored more than 50 journal articles, reports, and presentation abstracts. Her work included some of the first geologic maps of the Front Range, including the Big Thompson Canyon area (e.g., Boos and Boos, 1934). She dedicated a number of years mapping pegmatites around Storm Mountain (Boos, 1959a, 1959b). Based on this mapping (Boos, 1959a), she concluded that the pegmatites are related to the BTCt suite (referred to as the Mount Olympus granite at that time, see Boos and Boos, 1934). All are encouraged to read the biography of Margaret Fuller Boos found in Jacobson (1998).

No recent work has been done constraining the origin of the Hyatt pegmatite or other pegmatites in the area, but we believe that Boos (1959a) was correct in genetically relating the pegmatites to the BTCt. For at least the pegmatites around this portion of Storm Mountain Drive, the following lines of evidence suggest that one generation of pegmatites exists and they largely formed from a highly fractionated, incompatible and fluid-rich BTCt magma (see also Müller, 2019). These include (1) the spatial association of pegmatite and BTCt bodies (see above), (2) both the BTCt and pegmatites commonly form sills in the area, (3) both can display D_1 structures, and (4) tourmaline is found to either rim tonalite bodies (Stop 4B) or is commonly found as a pegmatite accessory mineral. However, this hypothesis requires testing as the pegmatites may have formed by anatexis (Webber et al., 2019), or some or all may have formed from fractionated melts associated with other plutonic suites, which has been shown to be the case for pegmatites in the Pikes Peak Granite (Raschke et al., 2021).

Stop 6. Glen Haven (Mahan et al., 2013)
(UTM NAD83 Zone 13T 462445, 4478187;
40.4535°N, 105.4429°W)

The town of Glen Haven was hit particularly hard by the 2013 flooding, and County Rd. 43 and the North Fork of the Big Thompson River were drastically modified in a number of locations, particularly in the Glen Haven migmatite outcrop described in Mahan et al. (2013). This outcrop is no longer accessible as the North Fork Big Thompson River now flows immediately along its base. However, road reconstruction created a number of new outcrops nearby that show similar features. To reach this new outcrop, drive 6.9 miles (11.1 km) northwest of Storm Mountain Road along County Rd. 43; a brand-new outcrop is on the north side of the road on the inside of a near hairpin turn.

In this new outcrop, granitic leucosome are typically parallel to gneissic layering, which is oriented 292, 65 NE. Within the migmatite zone, attributing outcrop fabrics to regionally recognized deformation phases can become complicated as fabric orientations are more variable. This is obvious when the structural data from Stop 6 of Mahan et al. (2013) are compared to this outcrop. Likely the gneissic layering is $S_{0/1}$ that has been reoriented by later deformations. Locally complex folding of leucosome and gneissic layers can be found and some leucosomes are rimmed by a thin biotite-rich selvage. Sillimanite nodules are also present. Obvious in this outcrop, and lacking in the original Stop 6 of Mahan et al. (2013), are less than 1-m-long felsic pegmatite bodies at a high angle to gneissic layering. Surrounding gneissic layering curves into some bodies. This, coupled with their orientation relative to the gneissic layering, suggests that pegmatite emplacement was late during the deformation event that helped develop the gneissic layering.

Stop 7. Granodiorite and Silver Plume Granite in the Upper Big Thompson Canyon
(UTM NAD83 Zone 13T 464290, 4471929;
40.3972°N, 105.4208°W)

From Stop 6, return to Drake, which is at the intersection of U.S. 34 and County Rd. 43. Turn right and travel SW along U.S. 34 for 6.1 miles (9.8 km), here U.S. 34 is oriented N-S. On the east side of the road is a large pull-off that provides easy access to two different rocks (Fig. 14).

Northeast of the parking area are many loose boulders and outcrops of Silver Plume granite (Fig. 14B). The Silver Plume granite can be highly variable in grain size and texture across the region, but here the rock is a medium-grained biotite-muscovite alkali feldspar granite. Sillimanite (fibrolite) is obvious in thin section, but matted aggregates are locally found in outcrop. Mica and feldspars are weakly aligned into what is believed to be a flow foliation; cm-scale biotite-rich xenoliths are locally common.

About 150 m to the south along U.S. 34 is a large road outcrop of granodiorite. U.S. 34 is often busy with fast moving traffic, so hike as far off the side of the road as possible. The rock here is a medium-grained biotite-quartz-feldspar rock. Distinguishing feldspars is difficult in outcrop except for the occasional pinkish alkali feldspar phenocryst, but thin section analysis confirms that plagioclase is by far the dominant feldspar, such that this is likely a true granodiorite. Trace muscovite is also present. A weak deformation fabric strikes NE-SW and dips moderately to the NW. Cross-cutting the granodiorite are a myriad of aplite to pegmatite veins and dikes consisting of muscovite, biotite, tourmaline, quartz, and feldspar.

The contact between the granodiorite and Silver Plume granite is visible in the road outcrop ~40 m north of the end of the parking area (Fig. 14A). Again, U.S. 34 is often busy with fast-moving traffic so stay as far off the road as possible. Here, some of the bodies of granodiorite appear as large angular xenoliths within the Silver Plume granite (Fig. 14C).

DISCUSSION

The Banda Sea in Indonesia has been used as a modern analog to amalgamation of the Yavapai and Mazatzal provinces (Jessup et al., 2005; Whitmeyer and Karlstrom, 2007). Key aspects of this model as applied to these provinces include the inferred occurrence of a collage of predominately juvenile islands arcs that sequentially accreted to the Wyoming Province at ca. 1.8–1.6 Ga. The vast majority of magmatic rocks are interpreted to have arc affinities, including evidence for bimodal magmatic rocks (see Jones et al., 2011). The turbidite deposits present in the Composite backarc have also been inferred to have formed in association with island arcs. The model recognizes that some accreted arcs may have associated pre–1.8 Ga crust, extensional backarc basins may have locally developed, and ocean currents may have carried old detritus great distances that was subsequently incorporated into arc magmas through subduction recycling; these are considered minor natural variations in the model (cf. Bickford et al., 2008).

Others have suggested that a simple juvenile arc accretion model does not adequately explain many observations. For example, whole rock Nd results from the GMA (Jones et al., 2011) and zircon U-Pb ages as old as the Archean and 1.9–1.8 Ga zircon Hf model ages from the Gunnison-Salida arc (e.g., Hill and Bickford, 2001; Bickford et al., 2008) are used to infer that these arcs were built upon a substrate of Trans-Hudson-Penokean (ca. 1.85 Ga) and older rocks. Additionally, the exposed ca. 1.84 Ga Elves Chasm granodiorite in the Grand Canyon (Hawkins et al., 1996) may reflect the presence of Trans-Hudson-Penokean crust there, but the recent work by Möller et al. (2017, 2020) suggests that old crust probably only locally occurs in central and northern Colorado.

Figure 15A summarizes key ages for the Poudre Basin. At ca. 1785–1770 Ma, both the GMA and Denver arc were active, though the Denver arc may be somewhat younger. Protoliths to the Poudre Canyon granitic gneiss and of the amphibolites both formed at this time as well (Workman, 2008; Table S2). However,

Figure 14. Granodiorite and Silver Plume granite at Stop 7. (A) Contact (outlined) between granodiorite and Silver Plume granite. Box shown in C. (B) Silver Plume granite close-up. (C) Granodiorite xenolith (outlined).

with only one age constraint and limited geochemistry, it is difficult to know if all amphibolite bodies are the same. All metasediment maximum depositional ages from the inferred extent of the basin fall in the range of ca. 1790–1730 Ma (Selverstone et al., 2000; Jones and Thrane, 2012; Müller, 2019). The oldest maximum depositional ages overlap with the age of the GMA and Denver arc, and emplacement of the protolith of the granitic gneiss and amphibolites. Therefore, the Poudre Basin appears to be no older than the age of the flanking arcs. The youngest maximum depositional ages overlap with the three youngest events, which themselves cannot be confidently distinguished by age, suggesting rapid transition from sedimentation to convergent tectonics. These youngest events include the ca. 1736 Ma intrusion of the BTCt (Fig. 7; Tables S5 and S6), the ca. 1731 Ma intrusion of the northern Front Range granodiorite (Fig. 7; Table S5), and the ca. 1725 Ma penetrative D_1 deformation (Müller, 2019; Ettsen, 2022).

The age of the basin is potentially a key data point that could be used to distinguish the two models. The juvenile arc accretion model requires the intra-arc basin to be older than the arcs, whereas the tectonic switching model requires the basin to be younger than the arcs. Based on the available data, the basin appears to have formed at essentially the same time as the arcs, with no evidence for a pre-arc age yet recognized (Fig. 15A). However, the oldest

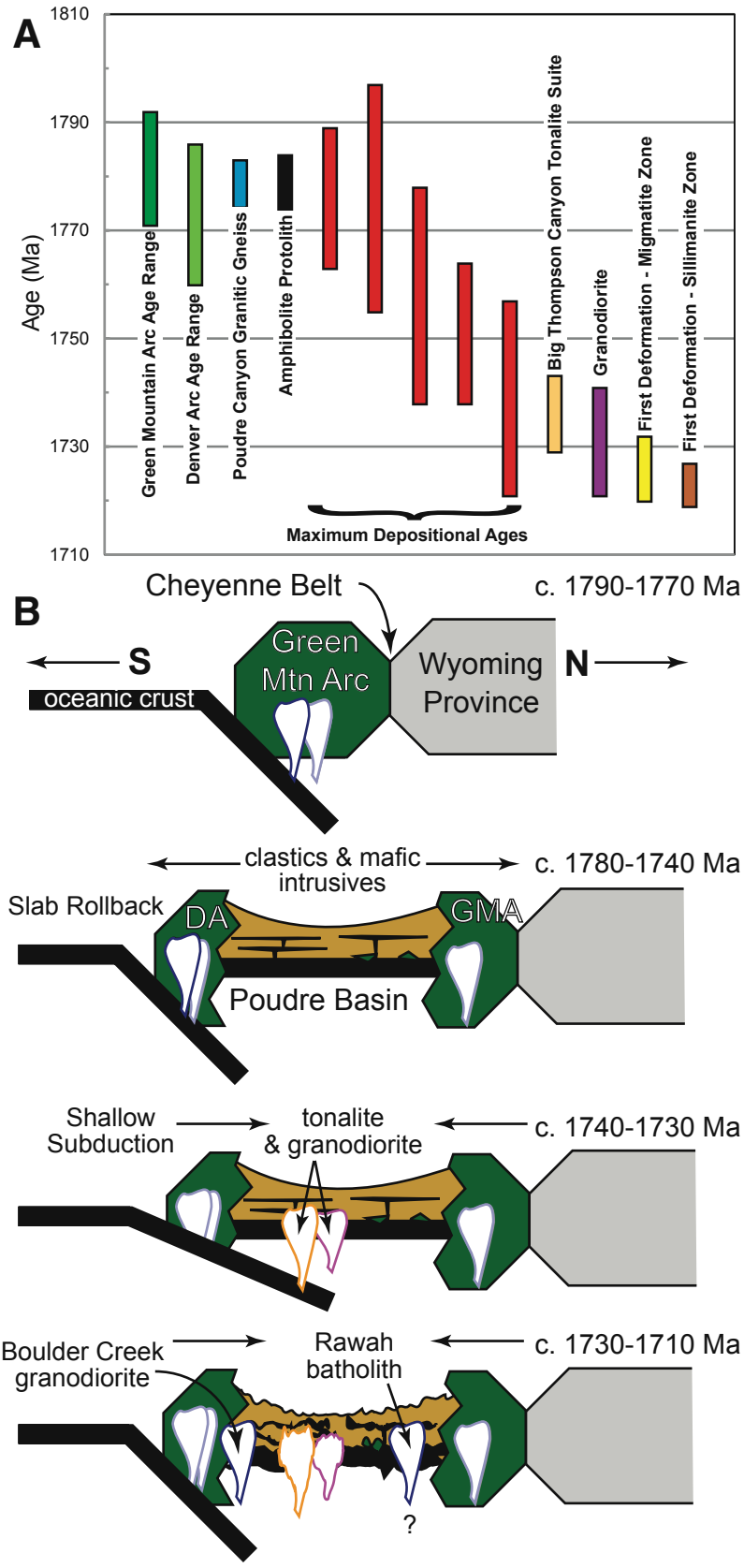

Figure 15. Summary of Paleoproterozoic tectonic events. (A) Timeline of major tectonic events within and immediately adjacent to the field-trip area. Text provides details regarding each event. (B) Schematic tectonic model based on the events show in A and other details discussed in the text. Based on models provided by DeWitt et al. (2010), Premo et al. (2010b), and Jones et al. (2010). DA—Denver arc; GMA—Green Mountain arc.

sediments may have been lost to subduction, or have not been sampled as of yet—the latter motivates future work.

The tectonic setting that generated the protoliths of the amphibolites cannot be determined definitively. Currently, the collective geochemistry presented suggests that a normal mid-ocean ridge setting is unlikely because the incompatible elements are quite enriched and show influence from a subduction zone. As no calc-alkaline igneous rocks typical of arc-related magmatism are associated with the amphibolites, this suggests that the amphibolites are not strictly arc-related and instead suggests their magma formed in an extensional backarc basin.

The adakite/TTG chemistry of the BTCt cannot uniquely be constrained to a single tectonic setting. However, given that the metamorphic geotherm had a relatively high *T*/*P* gradient (below aluminosilicate triple point), crustal thickness was likely never great enough to have resulted in eclogite melting at the base of the crust. Therefore, shallow subduction and partial melting of perhaps an oceanic plateau or seamount (e.g., Whattam and Stern, 2016) most likely generated the BTCt. Given that the northern Front Range granodiorite, essentially the same age as the BTCt, formed from a normal subduction zone but is spatially separated from the BTCt, this relationship can be explained by lateral variation in the slab depth controlled by the presence or absence of a plateau/seamount on the subducting slab. The plateau/seamount resulted in shallow subduction where the plateau/seamount partially melted to produce the BTCt. Elsewhere the subducting slab had more typical angles and depths and resulted in standard subduction zone mantle flux melts that produced the northern Front Range granodiorite. This, too, may explain the arcuate pattern of the approximately coeval $S_{0/1}$ foliation around the area where the BTCt is found—the plateau/seamount may have acted as an indenter during convergence.

Figure 15B summarizes a tectonic model for the region, which is based on the work of DeWitt et al. (2010), Premo et al. (2010b), and Jones et al. (2010) and explains the Poudre Basin as a collapsed backarc basin (see Cobbing and Pitcher, 1983; Collins, 2002; Kemp et al., 2009; Jones et al., 2010; Moscati et al., 2017). At ca. 1790–1770 Ma, the GMA formed during the Medicine Bow orogeny (Chamberlain, 1998), accreting to the Wyoming Province along the Cheyenne belt (Fig. 15B). At ca. 1780–1740 Ma, slab rollback caused the GMA to split, leaving the remainder of the GMA inactive while the other portion became the Denver arc. The Poudre Canyon granite gneiss is thought to be rifted portions of the GMA (Premo et al., 2010b). The Skin Gulch and the Idaho Springs–Ralston shear zones, the shear zones with the largest magnetic anomalies, may today mark the northern and southern limits, respectively, of extended arc crust at the margins of the Poudre Basin. As the Poudre Basin grew between the diverging arcs, it infilled with mostly clastic sediments generally derived from the arcs. Backarc basin mafic igneous rocks were emplaced, mostly as sills, into the basin. These rocks became the amphibolites that are now found throughout the northern Front Range. At ca. 1740–1730 Ma, sedimentation within the Poudre Basin ended with the initiation of shallow subduction caused by an oceanic plateau or seamount. Partial melting of the shallowly subducted plateau or seamount produced the BTCt magmas, while more deeply subducted portions of the slab that lacked the plateau/seamount produced the northern Front Range granodiorites. The plateau or sea mount acted as an indenter and drove D_1 that affected the region at ca. 1730–1720 Ma. Relatively high *T*/*P* metamorphism was synchronous, but outlasted deformation. Following deformation, subduction steepened and led to intrusion of the Boulder Creek granodiorite at ca. 1720–1710 Ma. The Rawah batholith is also of this age, and its location on the north side of the Poudre Basin suggests complexity in the number and/or geometry of subduction zones active at this time, consistent with Tyson et al.'s (2002) model for the Park Range.

This model focused on the Big Thompson–Poudre Canyons is quite consistent with data from the GMA. Extension within the GMA following its formation is marked by the intrusion of the ca. 1770–1755 Ma Horse Creek Anorthosite complex (Scoates and Chamberlain, 1997; Frost et al., 2000) and the ca. 1763 Ma Sierra Madre Granite and related rocks (Jones et al., 2010). Subsequent contraction and basin collapse occurs somewhat earlier within the GMA as evidenced by widespread ca. 1750 Ma contractional deformation (Jones et al., 2010).

Jones et al. (2009) and Jones and Thrane (2012) use an identical tectonic switching model to explain the occurrence of ca. 1700–1650 Ma, short-lived, extensional basin quartzite sequences found throughout the Yavapai and Mazatzal provinces. The model proposed here temporally extends the first cycle of tectonic switching back to ca. 1780 Ma, which together suggests that much of the crust of Colorado was formed and modified through tectonic switching processes from ca. 1780 Ma to ca. 1650 Ma.

ACKNOWLEDGMENTS

We acknowledge that this field guide discusses the geology of the ancestral lands of the Arapaho, Cheyenne, and Ute native peoples. Wayne R. Premo is thanked for his support of this research, access to data, thoughtful discussion regarding Colorado's Proterozoic geology, and providing comments on an early draft of this guide. Age and isotope work of samples provided by Wayne R. Premo was accomplished by the collection and analysis of a host of USGS field mappers during the USGS-funded Central Colorado Assessment Project. They include Karl Kellogg, Ed DeWitt, Terry Klein, Chris Friedrich, Jeremy Workman, Cal Ruleman, Bob Bohannon, Bruce Bryant, John "Jack" Reed, Wayne R. Premo, Richard J. Moscati, and Joseph L. Wooden (Stanford University SHRIMP-RG lab) among several others. Christopher Holm-Denoma is thanked for help with LA-ICP-MS operation. Richard Zaggle collected and partially processed some samples of the Big Thompson Canyon tonalite suite during undergraduate research at the University of Northern Colorado; Richard is also thanked for discussions regarding adakites/TTGs. Mark Jacobson is thanked for field assistance during field guide preparation and for his insights into the pegmatites of the

Storm Mountain area. Jane Selverstone and John Aleinikoff are thanked for discussions regarding their detrital zircon work. Jamey Jones and Kevin Chamberlain are thanked for providing reviews that help clarify and strengthen this contribution.

REFERENCES CITED

Abbott, J.T., 1976, Geologic Map of the Big Narrows Quadrangle, Larimer County, Colorado: U.S. Geological Survey Geologic Quadrangle Map GQ-1323, scale 1:24,000.

Aleinikoff, J.N., Reed, J.C., and Wooden, J.L., 1993a, Lead isotopic evidence for the origin of Paleo- and Mesoproterozoic rocks of the Colorado Province, U.S.A.: Precambrian Research, v. 63, no. 1–2, p. 97–122, https://doi.org/10.1016/0301-9268(93)90007-O.

Aleinikoff, J.N., Reed, J.C., and DeWitt, E., 1993b, The Mount Evans batholith in the Colorado Front Range: Revision of its age and reinterpretation of its structure: Geological Society of America Bulletin, v. 105, p. 791–806, https://doi.org/10.1130/0016-7606(1993)105<0791:TMEBIT>2.3.CO;2.

Allaz, J.M., Pritekel, C., Condit, C.B., Rattanasith, D., Mahan, K.H., Kelly, N.M., and Baird, G.B., 2015, Investigating the *P-T* conditions and temporal constraints on regional metamorphism near Big Thompson Canyon, Colorado, USA: Geological Society of America Abstracts with Programs, v. 47, no. 6, p. 11.

Allaz, J.M., Jercinovic, M.J., and Williams, M.L., 2020, U-Th-Pb total dating of REE-phosphate by electron microprobe: Review and progress: IOP Conference Series: Materials Science and Engineering, v. 891, 012001, https://doi.org/10.1088/1757-899X/891/1/012001.

Anderson, J.L., and Cullers, R.L., 1999, Paleo- and Mesoproterozoic granite plutonism of Colorado and Wyoming: Rocky Mountain Geology, v. 34, no. 2, p. 149–164, https://doi.org/10.2113/34.2.149.

Anderson, J.L., and Thomas, W.M., 1985, Proterozoic anorogenic two-mica granites: Silver Plume and St. Vrain batholiths of Colorado: Geology, v. 13, no. 3, p. 177–180, https://doi.org/10.1130/0091-7613(1985)13<177:PATGSP>2.0.CO;2.

Baird, G.B., Premo, W.R., Müller, S.R., Hooker, J.C., and Chumley, A.S., 2019, Constraining Paleoproterozoic timing and setting of deposition and tectonism in the Big Thompson and Rist Canyon areas, northern Colorado Front Range: Geological Society of America Abstracts with Programs, v. 51, no. 5, https://doi.org/10.1130/abs/2019AM-338542.

Bankey, V., Cuevas, A., Daniels, D.L., Finn, C.A., Hernandez, I., Hill, P.L., Kucks, R.P., Miles, W., Pilkington, M., Roberts, C., Roest, W.R., Rystrom, V.L., Shearer, S., Snyder, S., Sweeney, R.E., Velez, J., Phillips, J.D., and Ravat, D.K.A., 2002, Digital Data Grids for the Magnetic Anomaly Map of North America: U.S. Geological Survey Open-File Report 02-414, https://doi.org/10.3133/ofr02414.

Barovich, K.M., 1986, Age constraints on Early Proterozoic deformation in the northern Front Range, Colorado [M.S. thesis]: Boulder, Colorado, University of Colorado, 40 p.

Bennett, V.C., and DePaolo, D.J., 1987, Proterozoic crustal history of the western United States as determined by Nd mapping: Geological Society of America Bulletin, v. 99, p. 674–685, https://doi.org/10.1130/0016-7606(1987)99<674:PCHOTW>2.0.CO;2.

Bickford, M.E., and Hill, B.M., 2007, Does the arc accretion model adequately explain the Paleoproterozoic evolution of southern Laurentia?: An expanded interpretation: Geology, v. 35, no. 2, p. 167–170, https://doi.org/10.1130/G23174A.1.

Bickford, M.E., Van Schmus, W.R., and Zietz, I., 1986, Proterozoic history of the midcontinent region of North America: Geology, v. 14, p. 492–496, https://doi.org/10.1130/0091-7613(1986)14<492:PHOTMR>2.0.CO;2.

Bickford, M.E., Mueller, P.A., Kamenov, G.D., and Hill, B.M., 2008, Crustal evolution of southern Laurentia during the Paleoproterozoic: Insights from zircon Hf isotopic studies of ca. 1.75 Ga rocks in central Colorado: Geology, v. 36, no. 7, p. 555–558, https://doi.org/10.1130/G24700A.1.

Boos, M.F., 1959a, Pegmatites of Storm Mountain area, Larimer County, Colorado: Geological Society of America Bulletin, v. 70, no. 12, part 2, p. 1775.

Boos, M.F., 1959b, Pegmatites of Storm Mountain area, Larimer County, Colorado: Mining Engineering, v. 11, no. 12, p. 1227.

Boos, M.F., and Boos, C.M., 1934, Granites of the Front Range—The Longs Peak-St. Vrain Batholith: Geological Society of America Bulletin, v. 45, no. 2, p. 303–332, https://doi.org/10.1130/GSAB-45-303.

Bowring, S.A., and Karlstrom, K.E., 1990, Growth, stabilization, and reactivation of Proterozoic lithosphere in the southwestern United States: Geology, v. 18, no. 12, p. 1203–1206, https://doi.org/10.1130/0091-7613(1990)018<1203:GSAROP>2.3.CO;2.

Braddock, W.A., 1970, The Origin of slaty cleavage: Evidence from Precambrian rocks in Colorado: Geological Society of America Bulletin, v. 81, no. 2, p. 589–600, https://doi.org/10.1130/0016-7606(1970)81[589:TOOSCE]2.0.CO;2.

Braddock, W.A., and Cole, J.C., 1979, Precambrian structural relations, metamorphic grade, and intrusive rocks along the northeast flank of the Front Range in the Thompson Canyon, Poudre Canyon, and Virginia Dale areas (Field Trip 2), *in* Etheridge, F.G., ed., Northern Front Range and Northwest Denver Basin, Colorado: Geological Society of America Field Guide, Rocky Mountain Section, p. 106–121.

Braddock, W.A., Nutalaya, P., Gawarecki, S.J., and Curtin, G.C., 1970, Geologic Map of the Drake Quadrangle, Larimer County, Colorado: U.S. Geological Survey Geologic Quadrangle Map GQ-829, scale 1:24,000.

Braddock, W.A., Abbott, J.T., Connor, J.J., and Swann, G.A., 1988a, Geologic Map of the Poudre Park Quadrangle, Larimer County, Colorado: U.S. Geological Survey Geologic Quadrangle Map GQ-1620, scale 1:24,000.

Braddock, W.A., Connor, J.J., Swann, G.A., and Wohlford, D.D., 1988b, Geologic Map of the Laport Quadrangle, Larimer County, Colorado: U.S. Geological Survey Geologic Quadrangle Map GQ-1621, scale 1:24,000.

Braddock, W.A., O'Connor, J.T., and Curtin, G.C., 1989a, Geologic Map of the Buckhorn Mountain Quadrangle, Larimer County, Colorado: U.S. Geological Survey Geologic Quadrangle Map GQ-1624, scale 1:24,000.

Braddock, W.A., Calvert, R.H., O'Connor, J.T., and Swann, G.A., 1989b, Geologic Map of the Horsetooth Reservoir Quadrangle, Larimer County, Colorado: U.S. Geological Survey Geologic Quadrangle Map GQ-1625, scale 1:24,000.

Bucknam, R.C., and Braddock, W.A., 1989, Geologic Map of the Glen Haven Quadrangle, Larimer County, Colorado: U.S. Geological Survey Geologic Quadrangle Map GQ-1626, scale 1:24,000.

Cavosie, A., and Selverstone, J., 2003, Early Proterozoic oceanic crust in the northern Colorado Front Range: Implications for crustal growth and initiation of basement faults: Tectonics, v. 22, no. 2, https://doi.org/10.1029/2001TC001325.

Cawood, P.A., and Buchan, C., 2007, Linking accretionary orogenesis with supercontinent assembly: Earth-Science Reviews, v. 82, p. 217–256, https://doi.org/10.1016/j.earscirev.2007.03.003.

Cawood, P.A., Hawkesworth, C.J., and Dhuime, B., 2012, Detrital zircon record and tectonic setting: Geology, v. 40, no. 10, p. 875–878, https://doi.org/10.1130/G32945.1.

Cawood, P.A., Hawkesworth, C.J., and Dhuime, B., 2013, The continental record and the generation of continental crust: Geological Society of America Bulletin, v. 125, no. 1–2, p. 14–32, https://doi.org/10.1130/B30722.1.

Chamberlain, K.R., 1998, Medicine Bow orogeny: Timing of deformation and model of crustal structure produced during continent–arc collision, ca. 1.78 Ga, southeastern Wyoming: Rocky Mountain Geology, v. 33, no. 2, p. 259–277, https://doi.org/10.2113/33.2.259.

Chamberlain, K.R., and Mueller, P.A., 2019, Chapter 29—Oldest rocks of the Wyoming Craton, *in* Van Kranendonk, M.J., Bennett, V.C., and Hoffmann, J.E., eds., Earth's Oldest Rocks (2nd edition): Amsterdam, Elsevier, p. 723–739, https://doi.org/10.1016/B978-0-444-63901-1.00029-0.

Chumley, A.S., Baird, G.B., Kelly, N.M., Mahan, K.H., Zaggle, R.H., and Allaz, J.M., 2017, Geochemistry of the Big Thompson Canyon Paleoproterozoic granitoids, northern Colorado Front Range: Implications for tectonic activity and crustal growth at ~1.7 Ga: Geological Society of America Abstracts with Programs, v. 49, no. 5, https://doi.org/10.1130/abs/2017RM-293141.

Cobbing, E.J., and Pitcher, W.S., 1983, Andean plutonism in Peru and its relationship to volcanism and metallogenesis at a segmented plate edge, *in* Roddick, J.A., ed., Circum-Pacific Plutonic Terranes: Geological Society of America Memoir 159, p. 277–292, https://doi.org/10.1130/MEM159-p277.

Cole, J.C., 2004, Elegant simplicity in prograde-retrograde metamorphism of early Proterozoic metasediments, Front Range, Colorado: Geological Society of America Abstracts with Programs, no. 36, no. 5, p. 454.

Cole, J.C., and Braddock, W.A., 2009, Geologic Map of the Estes Park 30′ × 60′ Quadrangle, North-Central Colorado: U.S. Geological Survey Scientific Investigations Map 3039, 1 sheet + pamphlet, scale 1:100,000.

Collins, W.J., 2002, The nature of extensional accretionary orogens: Tectonics, v. 21, p. 6-1–6-12, https://doi.org/10.1029/2000TC001272.

Condie, K.C., 1982, Plate-tectonics model for Proterozoic continental accretion in the southwestern United States: Geology, v. 10, p. 37–42, https://doi.org/10.1130/0091-7613(1982)10<37:PMFPCA>2.0.CO;2.

Condie, K.C., 2005, TTGs and adakites: Are they both slab melts?: Lithos, v. 80, p. 33–44, https://doi.org/10.1016/j.lithos.2003.11.001.

Condie, K.C., 2013, Preservation and recycling of crust during accretionary and collisional phases of Proterozoic orogens: A bumpy road from Nuna to Rodinia: Geosciences, v. 3, p. 240–261, https://doi.org/10.3390/geosciences3020240.

Condie, K.C., and Kröner, A., 2013, The building blocks of continental crust: Evidence for a major change in the tectonic setting of continental growth at the end of the Archean: Gondwana Research, v. 23, p. 394–402, https://doi.org/10.1016/j.gr.2011.09.011.

Condie, K.C., and Martell, C., 1983, Early Proterozoic metasediments from north-central Colorado: Metamorphism, provenance, and tectonic setting: Geological Society of America Bulletin, v. 94, no. 10, p. 1215–1224, https://doi.org/10.1130/0016-7606(1983)94<1215:EPMFNC>2.0.CO;2.

Daniel, C.G., Pfeifer, L.S., Jones, J.V., III, and McFarlane, C.M., 2013, Detrital zircon evidence for non-Laurentian provenance, Mesoproterozoic (ca. 1490–1450 Ma) deposition and orogenesis in a reconstructed orogenic belt, northern New Mexico, USA: Defining the Picuris orogeny: Geological Society of America Bulletin, v. 125, no. 9–10, p. 1423–1441, https://doi.org/10.1130/B30804.1.

DePaolo, D.J., 1981, Neodymium isotopes in the Colorado Front Range and crust-mantle evolution in the Proterozoic: Nature, v. 291, p. 193–196, https://doi.org/10.1038/291193a0.

DeWitt, E.H., Premo, W.R., and Klein, T.L., 2010, The Early Proterozoic Poudre Basin, and important constraint of 1.77–1.73 Ga tectonic events in Northern Colorado: Geological Society of America Abstracts with Programs, v. 42, no. 5, p. 654.

Duebendorfer, E.M., Chamberlain, K.R., and Heizler, M.T., 2006, Filling the North American Proterozoic tectonic gap: 1.60–1.59-Ga deformation and orogenesis in southern Wyoming, USA: The Journal of Geology, v. 114, no. 1, p. 19–42, https://doi.org/10.1086/498098.

Duebendorfer, E.M., Williams, M.L., and Chamberlain, K.R., 2015, Case for a temporally and spatially expanded Mazatzal orogeny: Lithosphere, v. 7, p. 603–610, https://doi.org/10.1130/L412.1.

Erdman, M.E., Hacker, B.R., Zandt, G., and Seward, G., 2013, Seismic anisotropy of the crust: Electron-backscatter diffraction measurements from the Basin and Range: Geophysical Journal International, v. 195, no. 2, p. 1211–1229, https://doi.org/10.1093/gji/ggt287.

Ettsen, M., 2022, Timing of metamorphism, deformation, and anatexis of Big Thompson Canyon and Poudre Canyon area migmatites, Colorado Northern Front Range [M.S. thesis]: Greeley, Colorado, University of Northern Colorado, 118 p.

Evans, D.A.D., and Mitchell, R.N., 2011, Assembly and breakup of the core of Paleoproterozoic–Mesoproterozoic supercontinent Nuna: Geology, v. 39, no. 5, p. 443–446, https://doi.org/10.1130/G31654.1.

Frost, C.D., and Frost, B.R., 2011, On ferroan (A-type) granitoids: Their compositional variability and modes of origin: Journal of Petrology, v. 52, no. 1, p. 39–53, https://doi.org/10.1093/petrology/egq070.

Frost, C.D., Chamberlain, K.R., Frost, B.R., and Scoates, J.S., 2000, The 1.76-Ga Horse Creek anorthosite complex, Wyoming: A massif anorthosite emplaced late in the Medicine Bow orogeny: Rocky Mountain Geology, v. 35, no. 1, p. 71–90, https://doi.org/10.2113/35.1.71.

Frothingham, M.G., Mahan, K.H., Schulte-Pelkum, V., Caine, J.S., and Vollmer, F.W., 2022, From crystals to crustal-scale seismic anisotropy: Bridging the gap between rocks and seismic studies with digital geologic map data in Colorado: Tectonics, v. 41, no. 1, p. 1–24, https://doi.org/10.1029/2021TC006893.

Gable, D.J., 1980, The Boulder Creek Batholith, Front Range, Colorado: U.S. Geological Survey Professional Paper 1101, 86 p. + 2 plates, https://doi.org/10.3133/pp1101.

Gazel, E., Hayes, J.L., Hoernle, K., Kelemen, P., Everson, E., Holbrook, W.S., Hauff, F., van den Bogaard, P., Vance, E.A., Chu, S., Calvert, A.J., Carr, M.J., and Yogodzinski, G.M., 2015, Continental crust generated in oceanic arcs: Nature Geoscience, v. 8, p. 321–327, https://doi.org/10.1038/ngeo2392.

Gilkey, M.M., 1960, Hyatt Ranch Pegmatite, Larimer County, Colorado: U.S. Bureau of Mines Report of Investigations 5643, 18 p.

Godfrey, N.J., Christensen, N.I., and Okaya, D.A., 2000, Anisotropy of schists: Contribution of crustal anisotropy to active source seismic experiments and shear wave splitting observations: Journal of Geophysical Research–Solid Earth, v. 105, no. B12, p. 27,991–28,007, https://doi.org/10.1029/2000JB900286.

Hacker, B.R., Kelemen, P.B., and Behn, M.D., 2015, Continental lower crust: Annual Review of Earth and Planetary Sciences, v. 43, p. 167–205, https://doi.org/10.1146/annurev-earth-050212-124117.

Hanley, J.B., Heinrich, E.W., and Page, L.R., 1950, Pegmatite Investigations in Colorado, Wyoming and Utah, 1942–1944: U.S. Geological Survey Professional Paper 227, 125 p., https://doi.org/10.3133/pp227.

Hawkesworth, C.J., Cawood, P.A., Kemp, A.I.S., Storey, C., and Dhuime, B., 2009, A matter of preservation: Science, v. 323, p. 49–50, https://doi.org/10.1126/science.1168549.

Hawkesworth, C., Dhuime, B., Pietranik, A., Cawood, P., Kemp, A.I.S., and Storey, C., 2010, The generation and evolution of the continental crust: Journal of the Geological Society, v. 167, p. 229–248, https://doi.org/10.1144/0016-76492009-072.

Hawkins, D.P., Bowring, S.A., Ilg, B.R., Karlstrom, K.E., and Williams, M.L., 1996, U-Pb geochronology constraints on the Paleoproterozoic crustal evolution of the Upper Granite Gorge, Grand Canyon, Arizona: Geological Society of America Bulletin, v. 108, p. 1167–1181, https://doi.org/10.1130/0016-7606(1996)108<1167:UPGCOT>2.3.CO;2.

Hill, B.M., and Bickford, M.E., 2001, Paleoproterozoic rocks of central Colorado: Accreted arcs or extended older crust?: Geology, v. 29, no. 11, p. 1015–1018, https://doi.org/10.1130/0091-7613(2001)029<1015:PROCCA>2.0.CO;2.

Hooker, J., Baird, G.B., Chumley, A., and Müller, S., 2019, Paleoproterozoic igneous rocks of the Colorado Front Range as indicators of subduction zone processes during basin closure and accretion: Geological Society of America Abstracts with Programs, v. 51, no. 2, https://doi.org/10.1130/abs/2019SC-327683.

Hudson, M.E., Tracy, R.J., Munn, B.J., and Dahl, P.S., 2004, Timing of Proterozoic thermal events in the Poudre Canyon, Colorado Front Range; constraints from microprobe monazite U-Th-Pb dating: Geological Society of America Abstracts with Programs, v. 36, no. 5, p. 507.

Hutchinson, R.M., and Braddock, W.A., 1987, Precambrian structure, metamorphic mineral zoning, and igneous rocks in the foothills east of Estes Park, Colorado, *in* Beus, S.S., ed., Rocky Mountain Section of the Geological Society of America: Boulder, Colorado, Decade of North American Geology, Geological Society of America Centennial Field Guide 2, p. 303–306, https://doi.org/10.1130/0-8137-5402-X.303.

Irvine, T.N., and Baragar, W.R.A., 1971, A guide to the chemical classification of the common volcanic rocks: Canadian Journal of Earth Sciences, v. 8, p. 523–548, https://doi.org/10.1139/e71-055.

Jacobson, M.I., 1998, Margaret B. Fuller Boos: Colorado pegmatite geologist: Matrix (Hillerød), v. 6, no. 2, p. 73–81.

Jessup, M., Karlstrom, K.E., Connelly, J., Williams, M.L., Livaccari, R., Tyson, A., and Rogers, S.A., 2005, Complex Proterozoic Crustal Assembly of Southwestern North America in an Arcuate Subduction System: The Black Canyon of the Gunnison, Southwestern Colorado: American Geophysical Union Geophysical Monograph 154, 19 p., https://doi.org/10.1029/154GM03.

Johnson, T.E., Brown, M., Gardiner, N.J., Kirkland, C.L., and Smithies, R.H., 2017, Earth's first stable continents did not form by subduction: Nature, v. 543, p. 239–242, https://doi.org/10.1038/nature21383.

Jones, D.S., Snoke, A.W., Premo, W.R., and Chamberlain, K.R., 2010, New models for Paleoproterozoic orogenesis in the Cheyenne belt region: Evidence from the geology and U-Pb geochronology of the Big Creek Gneiss, southeastern Wyoming: Geological Society of America Bulletin, v. 122, no. 11–12, p. 1877–1898, https://doi.org/10.1130/B30164.1.

Jones, D.S., Barnes, C.G., Premo, W.R., and Snoke, A.W., 2011, The geochemistry and petrogenesis of the Paleoproterozoic Green Mountain arc: A composite(?), bimodal, oceanic, fringing arc: Precambrian Research, v. 185, no. 3–4, p. 231–249, https://doi.org/10.1016/j.precamres.2011.01.011.

Jones, J.V., III, and Thrane, K., 2012, Correlating Proterozoic synorogenic metasedimentary successions in southwestern Laurentia: New insights from detrital zircon U-Pb geochronology of Paleoproterozoic quartzite and metaconglomerate in central and northern Colorado, U.S.A.: Rocky Mountain Geology, v. 47, no. 1, p. 1–35, https://doi.org/10.2113/gsrocky.47.1.1.

Jones, J.V., III, Connelly, J.N., Karlstrom, K.E., Williams, M.L., and Doe, M.F., 2009, Age, provenance, and tectonic setting of Paleoproterozoic quartzite successions in the southwestern United States: Geological Society of America Bulletin, v. 121, no. 1–2, p. 247–264, https://doi.org/10.1130/B26351.1.

Karlstrom, K.E., and Bowring, S.A., 1988, Early Proterozoic assembly of tectonostratigraphic terranes in southwestern North America: The Journal of Geology, v. 96, no. 5, p. 561–576, https://doi.org/10.1086/629252.

Karlstrom, K.E., and Daniel, C.G., 1993, Restoration of Laramide right-lateral strike slip in northern New Mexico by using Proterozoic piercing points: Tectonic implications from the Proterozoic to the Cenozoic: Geology, v. 21, p. 1139–1142, https://doi.org/10.1130/0091-7613(1993)021<1139:ROLRLS>2.3.CO;2.

Karlstrom, K.E., and Houston, R.S., 1984, The Cheyenne Belt: Analysis of a Proterozoic suture in southern Wyoming: Precambrian Research, v. 25, p. 415–446, https://doi.org/10.1016/0301-9268(84)90012-3.

Karlstrom, K.E., and Williams, M.L., 2006, Nature of the middle crust—Heterogeneity of structure and process due to pluton-enhanced tectonism: An example from Proterozoic rocks of the North American Southwest, *in* Brown, M., and Rushmere, T., eds., Evolution and Differentiation of the Continental Crust: Cambridge, UK, Cambridge University Press, p. 268–295.

Karlstrom, K.E., Bowring, S.A., Chamberlain, K.R., Dueker, K.G., Eshete, T., Erslev, E.A., Farmer, G.L., Heizler, M., Humphreys, E.D., Johnson, R.A., Keller, G.R., Kelley, S.A., Levander, A., Magnani, M.B., Matzel, J.P., McCoy, A.M., Miller, K.C., Morozova, E.A., Pazzaglia, F.J., Prodehl, C., Rumpel, H.-M., Shaw, C.A., Sheehan, A.F., Shoshitaishvili, E., Smithson, S.B., Snelson, C.M., Stevens, L.M., Tyson, A.R., and Williams, M.L., 2002, Structure and evolution of the lithosphere beneath the Rocky Mountains: Initial results from the CD-ROM experiment: GSA Today, v. 12, no. 3, p. 4–10, https://doi.org/10.1130/1052-5173(2002)012<0004:SAEOTL>2.0.CO;2.

Karlstrom, K.E., Amato, J.M., Williams, M.L., Heizler, M., Shaw, C.A., Read, A.S., and Bauer, P., 2004, Proterozoic tectonic evolution of the New Mexico region: A synthesis, *in* Mack, G.H., and Giles, K.A., eds., The Geology of New Mexico: A Geologic History: Albuquerque, New Mexico, New Mexico Geological Society Special Publication 11, p. 1–34.

Karlstrom, K.E., Whitmeyer, S.J., Williams, M.L., Bowring, S.A., and Jessup, M.J., 2007, Does the arc-accretion model adequately explain the Paleoproterozoic evolution of southern Laurentia?: An expanded interpretation: Comment: Geology, v. 35, no. 1, p. e143–e144, https://doi.org/10.1130/G23971C.1.

Kelemen, P.B., and Behn, M.D., 2016, Formation of lower continental crust by relamination of buoyant arc lavas and plutons: Nature Geoscience, v. 9, p. 197–205, https://doi.org/10.1038/ngeo2662.

Kemp, A.I.S., Hawkesworth, C.J., Collins, W.J., Gray, C.M., Belvin, P.L., and EIMF, 2009, Isotopic evidence for rapid continental growth in an extensional accretionary orogen: The Tasmanides, eastern Australia: Earth and Planetary Science Letters, v. 284, p. 455–466, https://doi.org/10.1016/j.epsl.2009.05.011.

Lehman, M.R., 2020, U-Th-Pb monazite constraints on the timing of Paleoproterozoic metamorphism in Big Thompson Canyon, Colorado Front Range [M.S. thesis]: Golden, Colorado, Colorado School of Mines, 100 p.

Mahan, K.H., Allaz, J.M., Baird, G.B., and Kelly, N.M., 2013, Proterozoic metamorphism and deformation in the northern Colorado Front Range, *in* Abbott, L.D., and Hancock, G.S., eds., Classic Concepts and New Directions: Exploring 125 Years of GSA Discoveries in the Rocky Mountain Region: Geological Society of America Field Guide 33, p. 185–204, https://doi.org/10.1130/2013.0033(06).

Martin, H., 1993, The mechanisms of petrogenesis of the Archaean continental crust; comparison with modern processes: Lithos, v. 30, no. 3–4, p. 373–388, https://doi.org/10.1016/0024-4937(93)90046-F.

Martin, H., 1999, Adakitic magmas: Modern analogues of Archean granitoids: Lithos, v. 46, p. 411–429, https://doi.org/10.1016/S0024-4937(98)00076-0.

Möller, A., Premo, W.R., Baumgartner, L., Siron, G., Kooijman, E., and Kelly, N.M., 2017, A major Proterozoic terrane boundary in North America: Combined O_2-Lu/Hf-U/Pb analyses on magmatic zircon: Geological Society of America Abstracts with Programs, v. 49, no. 6, abstract 19-11.

Möller, A., Premo, W.R., Baumgartner, L., Siron, G., Kooijman, E., and Kelly, N.M., 2020, An integrated O_2-Hf-U/Pb isotope study of zircon on crustal growth in the Yavapai Province of Colorado: Goldschmidt Abstracts, https://doi.org/10.46427/gold2020.1822

Moscati, R.J., Premo, W.R., DeWitt, E.H., and Wooden, J.L., 2017, U-Pb ages and geochemistry of zircon from Proterozoic plutons of the Sawatch and Mosquito ranges, Colorado, U.S.A.: Implications for crustal growth of the central Colorado province: Rocky Mountain Geology, v. 52, no. 1, p. 17–106, https://doi.org/10.24872/rmgjournal.52.1.17.

Munn, B.J., and Tracy, R.J., 1992, Thermobarometry in a migmatitic terrane, northern Front Range, Colorado: Geological Society of America Abstracts with Programs, v. 24, no. 7, p. 264–265.

Munn, B.J., Tracy, R.J., and Armstrong, T.R., 1993, Thermobarometric clues to Proterozoic tectonism in the northern Front Range, Colorado: Geological Society of America Abstracts with Programs, v. 25, no. 6, p. 424–425.

Müller, S.R., 2019, Tectonic setting and timing of deformation in the Big Thompson Canyon, northern Colorado Front Range [M.S. thesis]: Greeley, Colorado, University of Northern Colorado, 65 p.

Nelson, B.K., and DePaolo, D.J., 1985, Rapid production of continental crust 1.7 to 1.9 b.y. ago: Nd isotopic evidence from the basement of the North American mid-continent: Geological Society of America Bulletin, v. 96, p. 746–754, https://doi.org/10.1130/0016-7606(1985)96<746:RPOCCT>2.0.CO;2.

Nesse, W.D., 1984, Metamorphic petrology of the northeast Front Range, Colorado: The Pingree Park area: Geological Society of America Bulletin, v. 95, no. 10, p. 1158–1167, https://doi.org/10.1130/0016-7606(1984)95<1158:MPOTNF>2.0.CO;2.

Nesse, W.D., and Braddock, W.A., 1989, Geologic Map of the Pingree Park Quadrangle, Larimer County, Colorado: U.S. Geological Survey Geologic Quadrangle Map GQ-1622, scale 1:24,000.

Niu, Y., Zhao, Z., Zhu, D., and Mo, X., 2013, Continental collision zones are primary sites for net continental crust growth—A testable hypothesis: Earth-Science Reviews, v. 127, p. 96–110, https://doi.org/10.1016/j.earscirev.2013.09.004.

Premo, W.R., and Fanning, C.M., 2000, SHRIMP U-Pb zircon ages for Big Creek gneiss, Wyoming and Boulder Creek batholith, Colorado: Implications for timing of Paleoproterozoic accretion of the northern Colorado province: Rocky Mountain Geology, v. 35, no. 1, p. 31–50, https://doi.org/10.2113/35.1.31.

Premo, W.R., and Van Schmus, W.R., 1989, Zircon geochronology of Precambrian rocks in southeastern Wyoming and northern Colorado, *in* Grambling, J.A., and Tewksbury, B.J., eds., Proterozoic Geology of the Southern Rocky Mountains: Geological Society of America Special Paper 235, p. 13–32, https://doi.org/10.1130/SPE235-p13.

Premo, W.R., Dewitt, E.H., Kellogg, K.S., Klein, T.L., Cole, J.C., and Workman, J.B., 2010a, Contrasting plutonic styles in the Paleoproterozoic of Colorado between ca. 1.725 to 1.690 Ga: Results from SHRIMP U-Pb zircon geochronology and major and trace-element geochemistry: Geological Society of America Abstracts with Programs, v. 42, no. 5, p. 654.

Premo, W.R., Klein, T.L., Kellogg, K., Cole, J.C., and Workman, J.B., 2010b, Some of the oldest rocks in Colorado are rift-related? Results from SHRIMP U-Pb zircon geochronology and major and trace-element geochemistry: Geological Society of America Abstracts with Programs, v. 42, no. 5, p. 42.

Ramsay, J.G., and Huber, M.I., 1983, The Techniques of Modern Structural Geology, Vol. 1: Strain Analysis: London, Academic Press, 307 p.

Raschke, M.B., Stern, C.R., Anderson, E.J.D., Skewes, M.A., Farmer, G.L., Allaz, J.M., and Persson, P.M., 2021, Bulk composition of a zoned rare-earth minerals–bearing pegmatite in the Pikes Peak granite batholith near Wellington Lake, central Colorado, USA: Rocky Mountain Geology, v. 56, p. 1–18, https://doi.org/10.24872/rmgjournal.56.1.1.

Reed, J.C., Jr., Bickford, M.E., Premo, W.R., Aleinikoff, J.N., and Pallister, J.S., 1987, Evolution of the Early Proterozoic Colorado province: Constraints from U-Pb geochronology: Geology, v. 15, p. 861–865, https://doi.org/10.1130/0091-7613(1987)15<861:EOTEPC>2.0.CO;2.

Reymer, A., and Schubert, G., 1986, Rapid growth of some major segments of continental crust: Geology, v. 14, p. 299–302, https://doi.org/10.1130/0091-7613(1986)14<299:RGOSMS>2.0.CO;2.

Scholl, D.W., and von Huene, R.E., 2009, Implications of estimated magmatic additions and recycling losses at the subduction zones of accretionary (non-collisional) and collisional (suturing) orogens, *in* Cawood, P.A., and Kröner, A., eds., Earth Accretionary Systems in Space and Time: Geological Society, London, Special Publication 318, p. 105–125, https://doi.org/10.1144/SP318.4.

Schulte-Pelkum, V., and Mahan, K.H., 2014, Imaging faults and shear zones using receiver functions: Pure and Applied Geophysics: Topical Volume on Crustal Fault Zones, v. 171, p. 2967–2991, https://doi.org/10.1007/s00024-014-0853-4.

Scoates, J.S., and Chamberlain, K.R., 1997, Orogenic to post-orogenic origin for the 1.76 Ga Horse Creek anorthosite complex, Wyoming, USA: The Journal of Geology, v. 105, p. 331–343, https://doi.org/10.1086/515928.

Selverstone, J., Hodgins, M., and Shaw, C., 1995, 1.4 versus 1.7 Ga metamorphism in the northern Colorado Front Range: A repeated history

of post-accretion midcrustal heating: Geological Society of America Abstracts with Programs, v. 27, no. 6, p. 49–50.
Selverstone, J., Hodgins, M., Shaw, C.A., Aleinikoff, J.N., and Fanning, C.M., 1997, Proterozoic Tectonics of the Northern Colorado Front Range: Denver, Colorado, Rocky Mountain Association of Geologists, Colorado Front Range Guidebook - 1997, p. 9–18.
Selverstone, J., Hodgins, M., Aleinikoff, J.N., and Fanning, C.M., 2000, Mesoproterozoic reactivation of a Paleoproterozoic transcurrent boundary in the northern Colorado Front Range: Implications for 1.7- and 1.4-Ga tectonism: Rocky Mountain Geology, v. 35, no. 2, p. 139–162, https://doi.org/10.2113/35.2.139.
Shah, A.A., and Bell, T.H., 2012, Ninety million years of orogenesis, 250 million years of quiescence and further orogenesis with no change in PT: Significance for the role of deformation in porphyroblast growth: Journal of Earth System Science, v. 121, no. 6, p. 1365–1399, https://doi.org/10.1007/s12040-012-0241-3.
Shaver, K.C., Nesse, W.D., and Braddock, W.A., 1988, Geologic Map of the Rustic Quadrangle, Larimer County, Colorado: U.S. Geological Survey Geologic Quadrangle Map GQ-1619, scale 1:24,000.
Shaw, C.A., and Karlstrom, K.E., 1999, The Yavapai-Mazatzal crustal boundary in the southern Rocky Mountains: Rocky Mountain Geology, v. 34, no. 1, p. 37–52, https://doi.org/10.2113/34.1.37.
Shaw, C.A., Snee, L.W., Selverstone, J., and Reed, J.C., Jr., 1999, $^{40}Ar/^{39}Ar$ thermochronology of Mesoproterozoic metamorphism in the Colorado Front Range: The Journal of Geology, v. 107, no. 1, p. 49–67, https://doi.org/10.1086/314335.
Shaw, C.A., Karlstrom, K.E., Williams, M.L., Jercinovic, M.J., and McCoy, A.M., 2001, Electron-microprobe monazite dating of ca. 1.71–1.63 Ga and ca. 1.45–1.38 Ga deformation in the Homestake shear zone, Colorado: Origin and early evolution of a persistent intracontinental tectonic zone: Geology, v. 29, no. 8, p. 739–742, https://doi.org/10.1130/0091-7613(2001)029<0739:EMMDOC>2.0.CO;2.
Shaw, C.A., Karlstrom, K.E., McCoy, A., Williams, M.L., Jercinovic, M.J., and Dueker, K., 2002, Proterozoic shear zones in the Colorado Rocky Mountains: From continental assembly to intracontinental reactivation, *in* Lageson, D., ed., Science at the Highest Level: Geological Society of America Field Guide 3, p. 102–117, https://doi.org/10.1130/0-8137-0003-5.102.
Sims, P.K., and Stein, H.J., 2003, Tectonic evolution of the Proterozoic Colorado province, southern Rocky Mountains: A summary and appraisal: Rocky Mountain Geology, v. 38, no. 2, p. 183–204, https://doi.org/10.2113/gsrocky.38.2.183.
Sims, P.K., Bankey, V., and Finn, C.A., 2001, Preliminary Precambrian Basement Map of Colorado—A Geologic Interpretation of an Aeromagnetic Anomaly Map: U.S. Geological Survey Open-File Report 01-0364, 1 plate, https://pubs.usgs.gov/of/2001/ofr-01-0364/.
Solway, D.R., 2014, Structural geology and metamorphism of the Skin Gulch area, northern Front Range, Colorado [M.S. thesis]: Flagstaff, Arizona, Northern Arizona University, 119 p.
Stern, R.J., and Scholl, D.W., 2010, Yin and yang of continental crust creation and destruction by plate tectonic processes: International Geology Review, v. 52, no. 1, p. 1–31, https://doi.org/10.1080/00206810903332322.
Sun, S.-s., and McDonough, W.F., 1989, Chemical and isotopic systematics of oceanic basalts: Implications for mantle composition and processes, *in* Saunders, A.D., and Norry, M.J., eds., Magmatism in the Ocean Basins: Geological Society, London, Special Publication 42, p. 313–345: Boston, Blackwell Scientific Publications, https://doi.org/10.1144/GSL.SP.1989.042.01.19.
Taylor, S.R., 1967, The origin and growth of continents: Tectonophysics, v. 4, no. 1, p. 17–34, https://doi.org/10.1016/0040-1951(67)90056-X.
Taylor, S.R., 1977, Island arc models and the composition of the continental crust, *in* Talwani, M., and Pitman, W.C., III, eds., Island Arcs, Deep Sea Trenches and Back-Arc Basins: Washington, D.C., American Geophysical Union, Maurice Ewing Series, v. 1, p. 325–335, https://doi.org/10.1029/ME001p0325.
Thurston, W.R., 1955, Pegmatites of the Crystal Mountain District, Larimer County, Colorado: U.S. Geological Survey Bulletin 1011, 185 p.
Tweto, O., 1979, Geologic Map of Colorado: U.S. Geological Survey, scale 1:500,000, https://doi.org/10.3133/70211263.
Tweto, O., and Sims, P.K., 1963, Precambrian ancestry of the Colorado Mineral Belt: Geological Society of America Bulletin, v. 74, p. 991–1014, https://doi.org/10.1130/0016-7606(1963)74[991:PAOTCM]2.0.CO;2.
Tyson, A.R., Morozova, E.A., Karlstrom, K.E., Chamberlain, K.R., Smithson, S.B., Dueker, K.G., and Foster, C.T., 2002, Proterozoic Farwell Mountain–Lester Mountain suture zone, northern Colorado: Subduction flip and progressive assembly of arcs: Geology, v. 30, p. 943–946, https://doi.org/10.1130/0091-7613(2002)030<0943:PFMLMS>2.0.CO;2.
Webber, K.L., Simmons, W.B., Falster, A.U., and Hanson, S.L., 2019, Anatectic pegmatites of the Oxford County pegmatite field, Maine, USA: Canadian Mineralogist, v. 57, p. 811–815, https://doi.org/10.3749/canmin.AB00028.
Whattam, S.A., and Stern, R.J., 2016, Arc magmatic evolution and the construction of continental crust at the Central American Volcanic Arc system: International Geology Review, v. 58, no. 6, p. 653–686, https://doi.org/10.1080/00206814.2015.1103668.
Whitmeyer, S.J., and Karlstrom, K.E., 2007, Tectonic model for the Proterozoic growth of North America: Geosphere, v. 3, no. 4, p. 220–259, https://doi.org/10.1130/GES00055.1.
Workman, J.B., 2008, Geologic Map of the Eaton Reservoir Quadrangle, Larimer County, Colorado, and Albany County, Wyoming: U.S. Geological Survey Scientific Investigations Map 3029, scale 1:24,000, https://pubs.usgs.gov/sim/3029/.
Workman, J.B., Cole, J.C., Shroba, R.R., Kellogg, K.S., and Premo, W.R., 2018, Geologic Map of the Fort Collins 30′ × 60′ Quadrangle, Larimer and Jackson Counties, Colorado, and Albany and Laramie Counties, Wyoming: U.S. Geological Survey Scientific Investigations Map 3399, 83 p., scale 1:100,000, https://doi.org/10.3133/sim3399.
Worthington, L.L., Miller, K.C., Erslev, E.A., Anderson, M.L., Chamberlain, K.R., Sheehan, A.F., Yeck, W.L., Harder, S.H., and Siddoway, C.S., 2016, Crustal structure of the Bighorn Mountains region: Precambrian influence on Laramide shortening and uplift in north-central Wyoming: Tectonics, v. 35, no. 1, p. 208–236, https://doi.org/10.1002/2015TC003840.

Manuscript Accepted by the Society 6 July 2022

Printed in the USA